AWARD NUMBER: W81XWH-20-1-0484

TITLE: Toward a Self-Administered Hearing Protection Regimen

PRINCIPAL INVESTIGATOR: Donna S. Whitlon

CONTRACTING ORGANIZATION: Northwestern University

REPORT DATE: OCTOBER 2023

TYPE OF REPORT: Annual

PREPARED FOR: U.S. Army Medical Research and Development Command
Fort Detrick, Maryland 21702-5012

REPORT DOCUMENTATION PAGE

Form Approved
OMB No. 0704-0188

1. REPORT DATE	**2. REPORT TYPE**	**3. DATES COVERED**
OCTOBER 2023	Annual	30SEPT2022 - 29SEPT2023

4. TITLE AND SUBTITLE

Toward a Self-Administered Hearing Protection Regimen

5a. CONTRACT NUMBER
W81XWH-20-1-0484

5b. GRANT NUMBER

5c. PROGRAM ELEMENT NUMBER

6. AUTHOR(S)

Donna S. Whitlon, Ph.D.

E-Mail: whitlon@northwestern.edu

5d. PROJECT NUMBER

5e. TASK NUMBER

5f. WORK UNIT NUMBER

7. PERFORMING ORGANIZATION NAME(S) AND ADDRESS(ES)

Northwestern University
633 Clark Street
Evanston, IL 60208

8. PERFORMING ORGANIZATION REPORT NUMBER

9. SPONSORING / MONITORING AGENCY NAME(S) AND ADDRESS(ES)

U.S. Army Medical Research and Development Command
Fort Detrick, Maryland 21702-5012

10. SPONSOR/MONITOR'S ACRONYM(S)

11. SPONSOR/MONITOR'S REPORT NUMBER(S)

12. DISTRIBUTION / AVAILABILITY STATEMENT

Approved for Public Release; Distribution Unlimited

13. SUPPLEMENTARY NOTES

14. ABSTRACT

This project aims to further both our basic understanding of the effects of different oral statins, with and without steroid drugs, on hearing loss and to compare the ability to protect hearing with the ability to protect hair cells and synapses within the cochlea. Concomitant with the laboratory studies we are undertaking a small, innovative clinical trial (randomized, double blind, prospective) to determine if the prevailing treatment (steroids) of idiopathic sudden sensorineural hearing loss (SSNHL) can be improved by adding a short course of statins. We are up and working despite having our laboratory moved for a second time in two years. This year we began to examine the ability of steroids given orally or IP to CBA/CaJ mice to protect against high level noise exposure (110 x 2 hr x 8-16 kHz). Thus far, none of our approaches have demonstrated any protective activity of the steroids on hearing thresholds. We also began accruing patients for our study of SSNHL. Thus far, we have one patient on the protocol who met all the inclusion and none of the exclusion criteria. This patient's hearing loss was severe but was completely reversed by whichever drug (randomized,double- blinded) received.

15. SUBJECT TERMS

Noise induced hearing loss, Statins, Sudden Sensorineural Hearing Loss, Clinical trial

16. SECURITY CLASSIFICATION OF:			**17. LIMITATION OF ABSTRACT**	**18. NUMBER OF PAGES**	**19a. NAME OF RESPONSIBLE PERSON**
					USAMRDC
a. REPORT	**b. ABSTRACT**	**c. THIS PAGE**			**19b. TELEPHONE NUMBER** *(include area code)*
U	U	U	UU	41	

TABLE OF CONTENTS

1. INTRODUCTION

This project aims to further both our basic understanding of the effects of different oral statins, with and without steroid drugs, on hearing loss, and to compare the ability to protect hearing with the ability to protect hair cells and synapses within the cochlea. Concomitant with the laboratory studies, we are undertaking a small, innovative clinical trial (prospective, randomized, double-blind) to determine if the prevailing treatment (steroids) for idiopathic sudden sensorineural hearing loss can be improved by adding a short course of an oral statin.

2. KEYWORDS

Noise induced hearing loss, statins, sudden sensorineural hearing loss, steroids, clinical trial

3. ACCOMPISHMENTS

What were the major goals of the project

	Percent Complete
Acquire IACUC approval and ACURO approval	100%
Validate new ABR measuring equipment	100%
Measure additional ABR of statins	60%
Statistics on ABR thresholds	Ongoing
Immunolabel all cochleas, count HC and synapses Statistics (above ABR study)	Ongoing
ABR study of Statin and Steroid and controls	Ongoing
Immunolabel all cochleas, count HC and synapses, statistics (statin+steroid ABR study)	Ongoing
Acquire Human Subjects Approval	100%
Acquire HRPO approval	100%
Hire and train clinical coordinator, put patient questionnaires on line, set up clinic for study	100%
Set up drugs at the pharmacy	100%
Initiate clinical trial, acquire data, calculate results	Initiated and enrolling
Begin writing paper on clinical Trial	X
Final calculations and final paper writing	X

What was accomplished under these goals?

Major Activities:

Once again, for the second time in two years, the University moved our entire floor to a new floor. Despite the delay it caused in our work, morale of the auditory group is noticeably higher than in the last couple of years. The new floor is large enough to accommodate all of the auditory researchers in the Otolaryngology Department. It is newly remodeled and has sufficient procedure rooms for all. Richter now has a large room with actual air flow that holds 4

sound booths and ABR equipment – one of them is my lab's. The entire floor is solely for the use of our auditory research group – 5 PIs and students and staff. People are interacting and collaborating. We have a seminar room where we and the other auditory scientists at the medical school meet weekly for journal club and to discuss research. The environment is very, very good and we are all moving ahead in our research.

The Whitlon lab's major activity has been in support of two major efforts. The first is preclinical animal work with auditory physiology measures, confocal microscopy and quantification. We are examining the effect of steroid – either dexamethasone or prednisolone – delivered either by gavage or IP on noise induced hearing loss (NIHL), eventually to be used as an adjunct to our statin therapy. This is the first group of experiments that we can identify anywhere in the literature that evaluates steroids on high decibel noise induced NIHL in CBA/CaJ mice. In fact, the evidence in the literature, however rare, is completely inconsistent in hearing insult (cisplatin, noise, strain of mouse, kanamycin) and in outcome measures (See Table 1). Our work, therefore, gives unique information.

MOUSE		**Insult**			
Tabuchi et al. 2006	ddy mice from Japan. 8 week old, outbred.	4 kHz pure tone, 128 dB for 4 hours	Methylprednisolone before or immediately after acoustic insult. *No report of the route of administration*	ABR before, immediately after, and 2 weeks after.	At two weeks, 100 mg/kg dose partially protects against threshold shift at 4,8 and 16 kHz
Hill et al., 2008	CBA/J, 1-2 months	Cisplatin	IT dexamethasone, 24 mg/ml; 5-10 µl. Five days. Saline in contralateral ear.	ABR; before and 8 days after IT.	After 8 days, some protection against threshold shift at 8 and 16 kHz, but not at 32 kHz.
Parham et al., 2011	CBA/J-NIA 24 month old	Cisplatin	IT injections of dexamethasone (24 mg/ml) or saline 5-10 µl.	ABR; pretreatment; after 8 days	After 8 days, show some protection at 24 and 32 kHz.
Fernandez and Lin, 2014	CBA/CaJ; 5-6 week old;	Kanamycin/ furosemide.	IP dexamethasone 1 hr before, 1,6,12,or 72 hr post insult.	Hair cell counts.	Pretreatment group with dexamethasone showed some improved counts compared to controls. Higher in basal and second turns. High variability
Han et al., 2015	C57/BL6 mice. 4 weeks of age	110 dB white noise centered at 10kHz. X 1 hr.	Dexamethasone IP (3 mg/kg/day on 5 consecutive days); compared to dexamethasone IT. Post noise days 1 and 4.	ABR and DPOAE. Before and immediately after noise and post noise day 7	Organ of Corti better preserved with IP route; OHC-efferent synapses better preserved in the IT group. ABR thresholds partially protected in both groups 8, 16 and 32 kHz. No protection DPOAE
Chen et al., 2019	C57/BL6; 8 week old	cisplatin	Dexamethasone loaded silk polyethylene hydrogel at the round window	ABR.	Protective effects against cellular ototoxicity, reactive oxygen species, partial hearing protection at 4,8 and 16 kHz
Cederroth et al., 2019	C57/BL6; males between 2-4 months	Noise; Broadband noise 6-12 kHz, 100 dB SPL for 1 hour.	4ml/kg IP of 0.5 mg/kg dexamethasone phosphate, 90 minute prior to noise	ABR	In a mouse model that exhibits circadian effects, dexamethasone was effective in protecting from acute noise only when given during the daytime.
Hughes et al., 2014	CBA/J; aged 8-10 weeks.	Cisplatin 3 mg/kg/day 5 days IP;	Dexamethasone IT daily for 5 days.	ABR. dexamethasone IT vs saline IT.	No statistically significant main effect of the drug on hearing.

Table 1. References to steroid, mouse and hearing loss: (references below)

Tabuchi et al. Therapeutic time window of methylprednisolone in acoustic injury. Otol. Neurotol (2006). 27:1176-1179.

Hill et al. Cisplatin-induced ototoxicity: effect of intratympanic dexamethasone injections. Otol Neurotol (2008). 29:1005-1011.

Parham. Can intratympanic dexamethasone protect against cisplatin ototoxicity in mice with age-related hearing loss? Otolaryngol Head Neck Surg (2011).145: 635-40.

Fernandes and Lin. Development of an ototoxicity model in the adult CBA/CaJ mouse and determination of a golden window of corticosteroid intervention for otoprotection. J. Otol. HNS. (2014). 43: 12

Hughes et al. Dexamethasone otoprotection in a multidose cisplatin ototoxicity mouse model Otol HNS. (2014) 150:115-20.

Han et al. Therapeutic effect of dexamethasone for noise induced hearing loss: systemic versus intratympanic injection in mice. Otol Neurotol (2015). 36:755-762.

Chen et al. Dexamethasone-loaded injectable silk-polyethylene glycol hydrogel alleviates cisplatin-induced ototoxicity. Int. J. Nanomedicine (219). 14:4211-4227.

Cederroth et al. Circadian regulation of cochlear sensitivity to noise by circulating glucocorticoids. Curr. Biol. (2019) 29:2477-2487.e6

Thus far, regardless of route (oral or IP), concentration or timing of drug delivery, neither dexamethasone (10, 20,25,50 mg/kg) nor prednisolone (0.625, 1.25, 2.5, 5 mg/kg, IP; 40, 20 10 5 mg/kg oral) protects against ABR threshold elevation in our CBA/CaJ mice under our noise conditions (110-112dB SPL x 2 hr x 8-16 kHz). Animals for each experiment are acclimated to our environment for 1 week, treated with steroid and noise the next week, ABR tested the next two weeks. We have seen occasional small improvements that are not reproducible.

We expected to see a protective effect on our noise induced ABR threshold shift, but thus far have not. It is interesting that there is still some controversy as to whether steroids are helpful as a treatment for human hearing loss. According to the Clinical Practice Guideline: Sudden Hearing Loss (update) [https://aao-hnsfjournals.onlinelibrary.wiley.com/doi/10.1177/0194599819859885] Statement 8: “Clinicians may offer corticosteroids as initial therapy to patients with SSNHL within 2 weeks of symptom onset”. “modest potential benefit”, “Aggregate evidence quality, grade C based on RCTs (randomized controlled trials) and systemic reviews of randomized trials downgraded for methodological limitations and again for inconsistent results” “Level of confidence in the evidence: Medium”.

Therefore, we are still in the research realm in determining the effects of corticosteroids on hearing loss. We will continue to study the steroids in our mouse model, but we intend to progress to different delivery methods: intratympanic, as is done clinically; possible intravenous and other approaches.

Our second major effort is directed towards a clinical trial of lovastatin+standard of care (methylprednisolone) vs standard of care in treatment of sudden sensorineural hearing loss (SSNHL). We were about 2 years delayed in the start of this study due to the pandemic. We opened the study in February. We find that the number of SSNHL patients is significantly fewer than those the hospital was seeing before the pandemic. It is possible that it indicates in general a slow return of the general population to medical care. Thirty three patients have been seen at Northwestern Hospital for SSNHL since our study began. In order to be rigorous and to provide usable information to our field, our unique study is a randomized, blinded study with many exclusion criteria. One patient, male, met all the inclusion and exclusion criteria. We do not know which of the treatments he received but his case is promising. He had a severe hearing loss (>50 dB at three frequencies) that was completely reversed with treatment.

In evaluating the possible reasons for patient accrual, the major causes of failure to meet the criteria are: Inclusion: Not diagnosed with one sided ISSNHL (24%); Seen in the clinic outside the required 2 week window (39%); Exclusion: Evidence of similar prior events (33.3); Use of statins within the last 12 months (30%); Oral steroid use within the last 30 days (45.5%). Given the pervasive use of statins in the population, we expected about 30% of the patients to be excluded by this criterion. The major issue appears to be that patients either delay going to a doctor or go to a local doctor or emergency room and have already failed treatment with a steroid. This looks to us to be an issue with advertising our study to the proper population. We are therefore developing ways to bring our study to the attention of the Chicago population. We deem it unrealistic to ask local doctors to give up their patients and refer to us for primary treatment in our study. Therefore, patients need to be properly educated on their own. The possibilities include advertising on hearing websites, making our own website that can pop up on search engines, etc.

Regardless our initial difficulties in patient recruitment, this study is immensely important in that it is rigorous, randomized and double-blinded, is prospective (something very rare in our field), and will give a definitive answer when it is completed. Will statins added to the standard of care yield a better outcome for SSNHL patients? A positive outcome in this study may also stimulate new studies of statins with other types of hearing loss.

What opportunities for training and professional development has the project provided.
The auditory group continues to have weekly journal club meeting where both students, faculty, and other staff are present. In addition, last year, this grant supported the attendance of my senior research associate to the ARO meetings, where he presented at a poster of his own work for his first time. Dr. Richter has mentored Dr. Depreux on the development of DPOAE and wave 1 measurements.

How were results disseminated to communities of interest?
Last year we published our work with statins in mice. We also have a paper under review that shows our new method for using lasers in the creation of cochleostomy in mice. Dr. Depreux presented his work at ARO.

What do you plan to do during the next reporting period to accomplish the goals?
1) Evaluate different ways of delivering steroids to the cochlea of mice to determine their effects on noise induced hearing loss with and without statins.
2) Develop an advertising approach to let our clinical study be known to a wider audience.
3) Continue to carry out immunolabeling, confocal imaging and quantification of hair cells and synapses in the cochleas from our physiology studies.

4. IMPACT

Most of the studies in the literature on statins and hearing are retrospective studies, so our prospective, randomized, double-blind study breaks new ground not only in the drug we are using, but also in the approach we are taking.

Our paper “Statins protect mice from high-decibel noise-induced hearing loss”, Depreux et al., was published in June 2023 in Biomedicine and Pharmacotherapy. It has been cited 4 times and according to Research Gate, has had 19 reads.

Our Paper “ALZET pump implantation in mice for chronic drug delivery”, Depreux et al., is still under review at Scientific Reports, but it was posted July 2023 as a preprint on Research Square. According to its site. It has been viewed 269 times and downloaded 5 times.

5. CHANGES/PROBLEMS

Changes in approach

Other than trying intraperitoneal delivery of steroids because oral delivery was not effective, there have been no changes approach

Actual or anticipated problems or delays and actions or plans to resolve them

Delay due to moving our lab to another floor for the second time in 2 years. We have now already recalibrated our equipment and done a number of physiological studies.

Steroids have not shown activity in protecting against high level induced hearing loss by gavage or by IP. We will move to different types of delivery such as intratympanic, which is a method that is already in clinical use.

There has been slow recruitment of patients for the clinical trial. We believe that to be a) because fewer SSNHL patients presented themselves at our hospital this year than in the years before the pandemic; b) A majority of patients are coming after initial treatment has already been attempted elsewhere; c) Some patients do not fall within the study window of two weeks from the start of the symptoms. To address these issues, we will improve our advertising outreach to the Chicago area. We cannot at this time increase the sites that are seeing patients, although several across the USA have asked to be included. It would take a larger cohort, new statistics, and passage through the IRB of Northwestern and of the Army.

6. PRODUCTS

Publications

Depreux, D., Czech, L., Young, H. Richter, CP, Zhou, Y., Whitlon, DS; .Statins protect mice from high-decibel noise-induced hearing loss. Biomedical Pharmacotherapy;163: 2023; 114674. Published. Federal support acknowledged.

Presentations

Depreux, F., Czech, L., Zhou, Y., Richter, C-P, Whitlon, D. Statins protect mice from noise-induced hearing loss. Association for Research in Otolaryngology, Abstracts. ARO 46th Annual Midwinter Meeting. Sat, February 11, 2023, Orlando Florida.

Depreux, F., Whitlon, D., Richter; C-P; ALZET pump implantation in mice for chronic drug delivery; Research Square. : https://doi.org/10.21203/rs.3.rs-3135966/v1. PREPRINT. Under review at Scientific Reports.

7. PARTICIPANTS AND OTHER COLLABORATING ORGANIZATIONS

	Project Role	Person-months	Contribution
Donna Whitlon Ph.D.	PI	8.4	Experimental design, writing, calculating, troubleshooting
Claus-Peter Richter, MD, Ph.D.	Co-investigator	No change	
Sumit Dhar, Ph.D.	Co-investigator	No change	
Alan Micco, MD	Physician, Co-investigator	No change	
Fred Depreux, Ph.D.	Senior Research Associate	10.5	ABR research
Yingjie Zhou, Ph.D.	Technician	2.4	Cochlea dissection
Aditi Argawal	Clinical Coordinator	3.6	Setting up documents, filtering patients, recruiting patients
Lyubov Czech	Research Tech II	10.5	Histology-immunolabeling, confocal, counting of synapses and hair cells

Change in active other support

Donna Whitlon, PI. ONR grant ended 12-31-22.

Appendix

Biomedicine & Pharmacotherapy 163 (2023) 114674

Contents lists available at ScienceDirect

Biomedicine & Pharmacotherapy

journal homepage: www.elsevier.com/locate/biopha

Statins protect mice from high-decibel noise-induced hearing loss

Frédéric Dépreux [a], Lyubov Czech [a], Hunter Young [a], Claus-Peter Richter [a,b,c], Yingjie Zhou [a], Donna S. Whitlon [a,b,d,*]

[a] Department of Otolaryngology-Head and Neck Surgery, Feinberg School of Medicine, Northwestern University, Chicago, IL 60611, USA
[b] Knowles Hearing Center, Northwestern University, Chicago, IL 60208, USA
[c] Department of Biomedical Engineering, Northwestern University, Chicago, IL 60208, USA
[d] Northwestern University Interdepartmental Neurosciences Program, Chicago, IL 60611, USA

ARTICLE INFO

Keywords:
Cochlea
HMG-CoA reductase inhibitor
ABR
Hair cells
Synapses
Noise-induced hearing loss

Chemical compounds studied in this article:
Fluvastatin (PubChem CID: 446155)
Lovastatin (PubChem CID: 53232)

ABSTRACT

No medical interventions for noise induced hearing loss (NIHL) are approved by the Food and Drug Administration (USA). Here, we evaluate statins in CBA/CaJ mice as potential drugs for hearing loss. Direct delivery of fluvastatin to the cochlea and oral delivery of lovastatin were evaluated. Baseline hearing was assessed using Auditory Brain Stem Responses (ABRs). For fluvastatin, a cochleostomy was surgically created in the basal turn of the cochlea by a novel, laser-based procedure, through which a catheter attached to a mini-osmotic pump was inserted. The pump was filled with a solution of 50 μM fluvastatin+carrier or with the carrier alone for continuous delivery to the cochlea. Mice were exposed to one octave band noise (8–16 kHz x 2 h x 110 dB SPL). In our past work with guinea pigs, fluvastatin protected in the contralateral cochlea. In this study in CBA/CaJ mice, hearing was also assessed in the contralateral cochlea 1–4 weeks after noise exposure. At two weeks post exposure, ABR thresholds at 4, 8, 12, 16, and 32 kHz were elevated, as expected, in the noise+carrier alone treated mice by approximately 9-, 17-, 41-, 29-, and 34-dB, respectively. Threshold elevations were smaller in mice treated with noise+fluvastatin to about 2-, 6-, 20-,12- and 12-dB respectively. Survival of inner hair cell synapses were not protected by fluvastatin over these frequencies. Lovastatin delivered by gavage showed lower threshold shifts than with carrier alone. These data show that direct and oral statin delivery protects mice against NIHL.

1. Introduction

Hearing loss is a pervasive, worldwide concern. Currently, as many as 430 million people (over 5% of the world's population (https://www.who.int/news-room/fact-sheets/detail/deafness-and-hearing-loss) live with a hearing loss that is severe enough to be considered disabling. In today's society, hearing loss can underlie difficulties in education and cognition, communication, job productivity, and integration into society.

In the hearing organ, the cochlea, sound vibrations are processed and encoded by the hair cells (the sensory cells). Signals representing the sound are transferred to the brain through the local, bipolar spiral ganglion neurons, where the information undergoes further analysis by higher auditory centers. Owing to the anatomy of the cochlea, sound frequencies are encoded in different regions of the organ, in a gradient from the base of the cochlear spiral, encoding mainly higher frequencies, to the apex, encoding lower frequencies.

A major cause of acquired hearing loss, a loss that occurs any time after birth, is exposure to incessant or loud noise that damages the cochlea. Sufficient loss of structure or function of hair cells or neurons or other cellular structures in the cochlea results in hearing impairment or deafness. When cells in the cochlea are damaged, medical treatment cannot depend on endogenous regeneration of hair cells and neurons because, in mammals, virtually none occurs. Medical interventions to prevent or repair hearing loss has largely had no or limited success. Only recently, in September 2022, sodium thiosulfate (Pedmark, Fennec Pharmaceuticals Inc.) was approved by the Food and Drug Administration to reduce the risk of ototoxicity associated with cisplatin in pediatric patients one month and older with localized, non-metastatic solid tumors. The drug is given intravenously at the time of cisplatin

Abbreviations: HMG-CoA, β-hydroxy β-methylglutaryl-coenzyme A; ABR, Auditory Brain Stem Response; DPOAE, Distortion Product Otoacoustic Emissions; NIHL, noise induced hearing loss; SPL, sound pressure level re 20 μPa; OHC, outer hair cell; IHC, inner hair cell.

* Correspondence to: Department of Otolaryngology, Feinberg School of Medicine, Searle, 10-521, 303, E Chicago Ave, Chicago, IL 60611, USA.
E-mail address: whitlon@northwestern.edu (D.S. Whitlon).

https://doi.org/10.1016/j.biopha.2023.114674
Received 24 January 2023; Received in revised form 1 April 2023; Accepted 6 April 2023
Available online 21 April 2023

treatment. The intravenous drug delivery makes it difficult for the drug to serve as a protective cure for a large population. An easily deliverable drug for hearing protection or restoration is still lacking.

With this in mind, in our past experiments, we focused on cochlear neuron (spiral ganglion) regeneration. The aim was to uncover new functions of known drugs that could be repurposed for the repair of neurites from damaged spiral ganglion neurons [1,2]. Our unique *in vitro* assay hit on the HMG-CoA reductase inhibitor class of drugs, statins, that are used in humans to reduce high serum cholesterol levels. We elevated fluvastatin to an *in vivo* study of spiral ganglion neurites in guinea pigs exposed to high level noise (120 dB SPL x 4 h x 4–8 kHz), which we knew to cause hearing damage and hair cell loss [3]. Rather than discover whether the drug would stimulate regeneration of damaged neurites in the absence of hair cell receptors, we found unexpectedly that fluvastatin delivered directly to one cochlea via a cochleostomy, protected against hearing loss in the contralateral cochlea and that the protection was associated with the retention of hair cells. At present, the molecular mechanism of fluvastatin's protection of hearing remains unknown.

One disadvantage of carrying out our earlier study in an outbred guinea pig model was the variability of individual guinea pig responses to noise exposure [4]. This variability was also reflected in the variability of fluvastatin hearing protection as measured by Auditory Brain Stem Response (ABR) thresholds. In the present study, we moved to an inbred mouse model, CBA/CaJ, in which changes in hearing after noise exposure are less variable [5]. The aim was to develop a model in which studies on molecular mechanisms of drugs that potentially protect from NIHL could be carried out. In this mouse model, we show that both fluvastatin directly delivered to the cochlea and orally dosed lovastatin protect against NIHL.

2. Materials and methods

2.1. Animals and ethical statement

Ten-week-old male CBA/CaJ mice were received from Jackson Laboratory (Bar Harbor, ME) and housed at the Northwestern Center for Comparative Medicine on the Chicago campus. Mice were allowed to acclimate to the new environment for at least one week before inclusion in the study. Experimental procedures required up to four additional weeks. Up to five animals were housed together in an autoclaved, individually ventilated cage of 36 cm (L) x 18 cm (W) x 12 cm (H). The room light was cycled 14 h on and 10 h off. Water and Teklad (Envigo, Indianapolis, IN) LM-485 Mouse/Rat sterilizable diet pellets were given ad libitum. All procedures were approved by Animal Care and Use Committee of Northwestern University following the National Academy of Sciences (USA) Guide for the Care and Use of Laboratory Animals [6] and by the Navy Bureau of Medicine and Surgery (BUMED).

2.2. Drugs

Fluvastatin sodium salt (Calbiochem, San Diego, CA) was dissolved in 100% Hybri-Max™ dimethyl sulfoxide (DMSO) (Millipore-Sigma, Merck KGaA, Darmstadt, Germany) at a concentration of 10 mM. Prior to filling the ALZET osmotic pump (Durect Corporation, Cupertino, CA, see below), fluvastatin solution was further diluted to a final concentration of 50 μM with 0.9% Sodium Chloride injection USP (Baxter, Deerfield, IL). The carrier without fluvastatin was prepared with a similar concentration of DMSO (0.5%) in 0.9% Sodium Chloride injection USP solution. For lovastatin (Sigma Aldrich, USP standard, St. Louis, Mo.) we tested several concentrations, carriers and delivery timings of lovastatin oral doses. The data here combines 60 mg/kg and 120 mg/kg regardless of carrier and timings. Timing of dosing ranged from daily 1–6 days before noise and for all, an hour before noise, an hour after noise and the day after noise exposure. Carriers tested were 1% propylene glycol, 0.1% Tween-80, 3% polyethylene glycol (PEG) 400 or 5% propylene glycol, 0.1% Tween-80, 30% PEG 400 (all carrier chemicals from Sigma Aldrich).

2.3. Noise exposure and sound levels

2.3.1. Fluvastatin

One hour after surgery recovery (animal sternal and ambulant), a single mouse was placed in a 9.5 cm diameter and 3.5 cm high circular, custom-made metallic mesh cage. The cage was placed in a sound-reduced chamber (66 cm (L) x 58 cm (W) x 51 cm (H); Industrial Acoustic Company, New York, NY) at a distance of 7.5 cm from the cage center to a JBL 2426 H Compression driver (JBL Professional, Northridge, CA) fixed above it. Two-inch, egg shape foam panels covered the inside of the chamber to reduce reverberations or standing waves. White noise electrical output was generated from the Hewlett Packard 33120A waveform generator (HP, Palo Alto, CA). The voltage command for the JBL 2426H compression driver was passed through a 90IB Frequency Devices filter (Frequency Device Inc., Ottawa, IL). The frequency band was 8–16 kHz, achieved with a programmable Butterworth H8B (−40 dB/octave) high pass filter and a Bessel L8L (−20 dB/octave) low pass filter. The combined frequency characteristics of the speaker and the filters was measured for our system and an example is shown in Supplemental Fig. 1.

The decrease in the sound level below 8 kHz and above 16 kHz was about 40 dB/ octave. The signal was then amplified with Hafler Transnova P1500 (Hafler, Port Coquitlam, Canada) and delivered to the JBL 2426H compression driver. Unanesthetized animals were exposed for 2 h at 110 dB SPL (SPL = sound pressure level referenced to 20 μPa). The sound level was measured using a 1/8″ pressure-field Brüel and Kjær microphone with the corresponding conditioning preamplifier (Brüel and Kjær, Nærum, Denmark). Before and after the mice were exposed to noise, the sound levels and corresponding frequency spectra were analyzed using custom-written software in MATLAB (MathWorks). Voltage commands for the speaker were also visually monitored on the screen of an Agilent 54624A oscilloscope (Agilent Technology, Santa Clara, CA) during the sound exposure for each mouse. Noise exposures were carried out between 10 AM and 5 PM.

2.3.2. Lovastatin

For the noise exposure in the lovastatin experiments, the metallic metal cage described above was divided into two sections separated by 1 cm so that two mice, one given lovastatin and one given carrier alone, could be noise-exposed at one time. The cage was placed in a sound-reduced chamber (66 cm (L) x 66 cm (W) x 70 cm (H) at a distance of 8 cm from the cage center to a 950NeoPB 8 ohms compression driver (Radian Audio Engineering, Pomona, CA). Two-inch, egg-shape foam panels covered the inside of the chamber to reduce reverberations or standing waves. White noise electrical output was generated from the Hewlett Packard 33120A waveform generator (HP, Palo Alto, CA). The voltage command for the 950NeoPB compression driver was passed through a 90IB Frequency Devices filter (Frequency Device Inc., Ottawa, IL). The frequency band was 8–16 kHz, achieved with a programmable Butterworth H8B (−40 dB/octave) high pass filter and a Bessel L8L (−20 dB/octave) low pass filter. The combined frequency characteristics of the speaker and the filters was measured for our system and an example is shown in Supplemental Fig. 1. The decrease in the sound level below 8 kHz and above 16 kHz was about 40 dB/ octave. The signal was then amplified with Crown 2002 XTi amplifier (Harmon, Elkhart, IN) and delivered to the 950NeoPB compression driver. Unanesthetized animals were exposed for 2 h at 110 dB SPL. The sound level was measured using a 1/8″ pressure-field Brüel and Kjær microphone with the corresponding conditioning preamplifier (Brüel and Kjær, Nærum, Denmark). Before and after the mice were exposed to noise, the sound levels and corresponding frequency spectra were analyzed using custom-written software in MATLAB (MathWorks). Voltage commands for the speaker were also visually monitored on the screen of an Siglent SDS 1104XE oscilloscope (Siglent Technologies, Solon, OH) during the

sound exposure for each mouse. Noise exposures were carried out between 10 AM and 5 PM.

2.4. Validation of the physiologic setup and speaker system for mouse NIHL experiments

Using octave band noise (8–16 kHz x 2 h; frequency spectrum depicted in Supplemental Fig. 1, we carried out a limited dose/response study over four weeks to determine the effects of measured sound pressure level on ABR thresholds in our setup. Supplemental Fig. 2 demonstrates the ABR threshold elevations at noise levels 90-, 95-, 100-, 105-, and 110-dB SPL.

Octave band noise (8–16 kHz) delivered for 2 h elevates the ABR thresholds at levels related to the noise level. Of importance is that the elevated ABR thresholds were stable by one week after noise exposure, and there was no further elevation of the ABR thresholds in the ensuing 2, 3, and 4 weeks. Thus, a permanent threshold was established by one week after noise exposure at all tested sound levels. We also determined ABR thresholds 24 h after noise exposure at 90- and 95- dB SPL. At 95 dB SPL, there was a significant temporary threshold shift (TTS) at 24 h that was not observed one week after noise exposure. Based on these data, we chose 110 dB SPL as our high-level noise exposure stimulus for our system.

2.5. Cochleostomy and osmotic pump implantation

For fluvastatin, we used a protocol for cochleostomy, and osmotic pump implantation adapted from that we used for guinea pig [3], with improvements for the smaller cochlea and the assistance of a surgical CO_2 laser (Sharplan 20 C, Sharplan, Allendale, NJ).

Specifically: A biocompatible, custom-made catheter was constructed using two different diameters medical grade tubings sealed together with silicone. One was a polyimide tube of 100 μm inner diameter (ID) and 132 μm outer diameter (OD) (Generous gift of Microlumen, Oldsmar, FL), and the other, a TYGON™ tube of 1 mm ID and 1.2 mm OD (Tygon Saint-Gobin USA, Malvern, PA). Forty-eight hours after recording baseline ABR thresholds and 90 min before surgery, the animals received intraperitoneally (i.p.) a dose of 0.05 mg/kg Buprenex (Reckitt Benckiser Group, Slough, UK), followed thirty minutes later by a subcutaneous injection of 1 ml of 0.9% Sodium Chloride USP grade. Anesthesia was induced by exposing the animal to 3% isoflurane under oxygen in an induction chamber and was then maintained during the surgery with 1–3% of isoflurane in oxygen given via a nose cone. To implant the pump into the right ear, the mouse was positioned on its back to perform a longitudinal, ventral, para-medial skin incision from the angle of the right mandible toward the right front leg. After surgically exposing the bulla, the middle ear was opened with either sharp forceps or the combination of the CO_2 laser, equipped with an OTO laser fiber from Omniguide (Omniguide, Lexington, MA) and sharp forceps. The laser was operated in single pulse mode of 100 ms and 5 Watts power. The cochleostomy was then created in the cochlear base, close to the stapedial artery and the round window, using either an electric drill (OmniDrill35, World Precision Instruments, Sarasota, FL) or the CO_2 laser in single pulse mode, 100 ms pulse length at 7 Watts power.

The drug solution (fluvastatin in a carrier solution) or carrier alone was loaded into an ALZET micro-osmotic pump (Model 1004, 0.11 μl/h, up to 28 days: Durect Corporation, Cupertino, CA) using a filling tube. The custom-made catheter was flushed with the same solution and inserted into the pump. A cavity was created under the skin, extending beyond the animal's shoulder and back, between the skin and the muscle fascia. The pump was then inserted towards the shoulder blades. The sternocleidomastoid muscle was elevated to create a tunnel to allow the passage of the polyimide tubing portion of the catheter. The tip was lightly bent, inserted into the scala tympani through the cochleostomy, and sealed to the bulla with dental acrylic. The ALZET pump was then held in its final position with subcutaneous tissues using a 6–0 biodegradable suture (Ethicon, Johnson & Johnson Company, New Brunswick, NJ) along the upper right side of the animal thoracic cage. Finally, the skin was closed in two layers. The first with a 6–0 biodegradable suture, the second with a 6–0 non-degradable suture (Ethicon). The mouse was then placed on its back on top of a heating pad in a recovery box and monitored until it was sternal and ambulant. Post-surgical pain was managed by 0.05 mg/kg Buprenex IP, administered every 12 h for 48 h. Mice were then individually housed for the rest of the study.

2.6. Gavage and lovastatin delivery

Mice were weighed to determine the volume of drug and gavage buffer. A 26-gauge stainless steel needle was mounted to a 1 ml syringe (Becton Dickinson, Franklin Lake, NJ) and the liquid was taken up. The needle was then introduced to the region of the stomach by the mouth and the liquid flushed quickly. Animals were placed back into the cage and monitored for an hour prior to being noise exposed or brought back to the animal facility.

2.7. Auditory brainstem responses (ABRs)

2.7.1. General approach

Cochlear ABRs were measured after one week of acclimation to the animal rooms and 48 h before the pump implantation and noise exposure (fluvastatin) or noise exposure (lovastatin)- (the "baseline"). ABR measurements were repeated weekly in the cochlea contralateral to the surgically modified cochlea [3] up to four weeks post-implantation. In a few cases, ABRs were recorded 24 h after noise exposure to determine the sound pressure level at which a temporary threshold shift was observed. Mice were placed under anesthesia via IP injection of a mixed solution of Ketamine (100 mg/kg; Covetrus, Dublin, OH) and Xylazine (10 mg/kg; Akom Animal Health Inc., Lake Forest, IL) in 0.9% USP grade saline. Three hypodermic needles were inserted under the skin of an anesthetized mouse, one at the ipsilateral mastoid bone (high), one at the vertex (low), and one reference electrode under the skin at the animal's lower back (common ground).

2.7.2. Fluvastatin study

A custom-made speculum attached to a Beyer 770 Pro headphone driver (Bayerdynamics, Farmingdale, NY) was placed at the opening of the outer ear canal of the left ear. Voltage commands for pure tone stimuli (7 ms in length, including a 2 ms rise and fall time) were generated with a computer I/O board (KPCI 3110; Keithley, Tektronix, INC., Beaverton, OR) and custom-written software in TestPoint [3].

The carrier frequencies were 32, 16, 12, 8, and 4 kHz. The phase of the pure tone carrier was alternated between 0 and 180 degrees. Stimuli were presented at a rate of about 4 Hz. The voltage command for the stimuli was passed through an attenuator (Model 8310–35–2-F; 0–100 dB; Weinschel Corp., Frederick, MD) to adjust the output voltage, which controls an audio amplifier (the maximum output was limited to 1 V_{rms}) driving a Beyer DT770 Pro headphone speaker. The attenuation was changed in steps of 5 dB. The peak sound level for the acoustic stimuli was determined by placing the opening of the speaker speculum in front of the protective grid of the 1/8-inch microphone (Brüel & Kjær North America Inc. Norcross, GA). The maximum sound levels of the speaker at 32, 16, 12, 8, and 4 kHz was 73-, 88,- 94-, 100-, and 84- dB SPL respectively.

Pure tone burst evoked potentials were band pass filtered, 0.3–3 kHz (filter slopes −12 dB/octave), amplified 10,000 times by a preamplifier (ISO80, World Precision Instruments, Sarasota, FL), filtered by the 90IB Frequency Devices filter (0.3–3 kHz, high pass filter slope = −40 dB/octave, low pass filter slope = −20 dB/octave, gain 20 dB) and recorded by the PC via the KPCI 3110 I/O board. Using a custom-written software (CPR) with trial rejection [3], up to 1024 responses from the tone bursts were averaged. Evoked ABR waveforms were imaged on the PC monitor

screen, and the computer software saved the data for each attenuation.

Evoked potential waveforms (ABRs) were generated and recorded by delivering pure tone bursts at the maximal intensity of the speaker at each pure tone frequency and decreasing by 5 dB SPL until the evoked potential waveforms disappeared to the electrical noise floor. That sound level was defined as the "threshold".

2.7.3. Lovastatin study

ABRs in the lovastatin study were determined with a commercially available ABR recording system RZ6 Multi I/O processor (Tucker-Davis Technologies: TDT, Alachua, FL). Mice were anesthetized by an intraperitoneal injection of a Ketamine / Xylazine hydrochloride (100 mg/kg / 10 mg/kg) solution.

The speculum of MF1 Multi-Field Magnetic Speaker (Tucker-Davis Technologies: TDT, USA) was placed at the entry of the external outer ear canal. The MF1 speaker calibration was perform using a 378C01 microphone system (PCB Piezotronics, Depew, NY), composed of a ¼" PCB 377C01 microphone, a pre-amplifier PCB 426B03, and the 482C02 battery-powered conditioning amplifier. The conditioning amplifier gain was at 1. The microphone was placed at the tip of the MF1 speaker speculum. The maximal sound pressure for all frequencies was set to 90 dB SPL in the BioSigRZ software (Tucker-Davis Technologies). The speaker corrections were saved and were used for all ABR recordings.

Voltages between the needle electrodes were measured with the Medusa4Z, the system's preamplifier and analog-to-digital (A/D) converter. The A/D conversion rate was set to 25 kHz. The data acquisition started with measuring the electrode's impedance, which was typically about 1 kΩ. The signal from the Medusa4Z was software filtered using a bandpass (0.3–3 kHz) and a notch filter at 60 Hz. The Medusa preamplifier was connected via optical cable to the RZ6 Multi I/O processor input. Sound evoked ABR waveforms were displayed via the BioSigRZ software. The voltage command for pure tone stimuli was generated by the RZ6 Multi I/O processor controlled by the BioSigRZ software. The voltage command was directly delivered to the MF1 Multi-Field Magnetic Speaker. The data acquisition time was 40 ms, with a 5 ms single channel cosine-square gated tone followed by 35 ms quiet segment. The carrier frequencies were 32, 16, 12, 8, and 4 kHz. The phase of the pure tone carrier was alternated between 0 and 180 degrees to reduce contributions by the cochlear microphonics. Stimulus presentation was at a rate of 21 Hz for averaging. A total of maximum 512 responses was averaged. The pure tone level was decreased from 90 to 20 dB SPL in 5 dB steps. BioSigRZ's trial rejection feature removed trials with large voltage amplitudes, unrelated to the ABR response. At the conclusion of the measurements, data were saved and exported for further analysis using custom written MATLAB code.

2.7.4. Threshold determination

Recorded ABR responses were graphed for visual analysis. To determine the threshold with the computer, the average root means squared amplitude in a 10 ms window at the beginning of the recording (target window) containing the APR response to the acoustic stimulus was compared with a similar sized window (reference window) at the end of the recording (quiet region). The amplitudes obtained for the two windows were plotted. Traces for target and the reference window were each interpolated at a 200-point resolution. The resulting 2 traces were compared, and threshold was defined as the rms-amplitude in the target window equal or smaller that the amplitude in the 1.1-times the amplitude in the reference window. We confirmed the computer-generated thresholds by visual inspection of the plots.

Initially, ABR thresholds were determined at 32, 16, 8, 4, and 2 kHz. In later experiments, ABR thresholds were no longer determined at 2 kHz but at 12 kHz instead. Hence, fewer animals were tested at 12 kHz. Data captured at 12 kHz was included on the threshold shift graphs but not for statistical calculations. Threshold shifts were determined by subtracting the baseline threshold from that recorded after noise exposure. Threshold shifts were determined for each animal, then averaged within experimental groups.

ABR thresholds in the fluvastatin+carrier-treated and carrier alone-treated mice were measured weekly. Noise alone and unexposed treated mice were measured at various week intervals. Not all mice were maintained for the entire 4 weeks.

2.8. Cochlea fixation and decalcification

Immediately after the last ABR recording, each animal was euthanized by intraperitoneal injection of 0.1 ml/mouse of EUTHASOL® Euthanasia pentobarbital solution (390 mg/ml pentobarbital sodium, 50 mg/ml phenytoin sodium; Virbac Corporation, Westlake, TX). Intracardiac perfusion of 4% paraformaldehyde (PFA) in 0.1 M sodium phosphate (pH 7.4) was performed, and both temporal bones were excised. The bulla and ossicles were removed, round and oval cochlear windows were opened, and the bony capsule was perforated at the cochlear apex to allow adequate tissue fixation for one hour at room temperature (RT). Cochleas were then washed in phosphate-buffered saline (PBS, pH 7.4). Cochleas were transferred to 10% EDTA in PBS (pH 7.4) for decalcification for two days on a rotator at 4 °C. Cochleas were stored in 0.25% PFA in PBS at 4 °C until processed for histology.

2.9. Dissection and immunostaining of the cochlea

Decalcified cochleas were dissected into three turns, according to Montgomery and Cox (2016) [7]. The tissue was cryoprotected in 30% sucrose for 15 min and frozen at − 80°C to permeabilize [8]. The pieces were thawed, incubated 15 min at room temperature in phosphate-buffered saline (PBS; pH 7.3), then in a blocking reagent (5% Normal Donkey Serum (NDS) with 0.3% Triton-X 100 in PBS) for 1 hr. Next, the tissue was incubated at 37 °C for 24 h in the primary antibody diluted in the 0.3% NDS and 0.3% Triton buffer. Primary antibodies: To visualize presynaptic ribbons, mouse (IgG1) anti $CTBP_2$ (C-terminal binding protein 2; BD Transduction labs, 1:200); to label glutamate receptor patches, mouse (IgG2) anti-GluA2 (GluA2, Millipore #MAB397, 1:500); to label hair cells, rabbit anti myosin VIIa (Proteus #25–6790, 1:200) [9]. Before incubation in secondary antibody, turns were washed three times in 1x PBS and then incubated for 2 h at 37 °C in species-appropriate secondary antibodies: Goat anti-Mouse IgG1 Cross-Adsorbed Alexa Fluor 568 (ThermoFisher, A21124), Goat anti-Mouse IgG2a Cross-Adsorbed Secondary Antibody Alexa Fluor 488 (ThermoFisher, A21131) and F(ab) Fragment Donkey anti-rabbit IgG (H+L)-AF647 (Jackson cat 711–606–152).

2.10. Imaging

Inner hair cell (IHC) synaptic zones were imaged with Nikon A1 confocal microscope (Center for Advancing Microscopy\Nikon Imaging Center at the Northwestern University) with 488-nm and 561-nm, and 640-nm lasers for excitation. Images were sampled with 0.21 μm/pixel using a Plan Apo 100x oil-immersion objective, NA 1.45, and a z-step size of 0.3 μm. *Z*-stacks were captured through the entire depth of the organ of Corti and from the base to the apex. Each stack encompassed from 12 to 16 IHCs depending on angle and location. The same microscope was used for outer hair cell (OHC) imaging using a Plan Apo 60x oil-immersion objective and NA 1.40 with 0.36 μm/pixel. Low-power DIC large images of each dissected piece of the cochlea were taken with a Nikon Ti2 Widefield microscope (S Plan Fluor ELMD 20X Ph1 ADM and NA 0.45 with 36 μm/pixel). Advanced image stitching with Nikon NIS elements was used to create the whole cochlear turn images. These images were used to construct the cochlea frequency map using a custom plug-in to ImageJ: (http://www.masseyeandear.org/research/ent/eaton-peabody/epl-histology-resources).

2.11. Image analysis

Bitplane "Surfaces "analysis was used to quantify the labeled cell's pre-synaptic and post-synaptic components. Confocal z-stacks were imported to image-processing IMARIS 9.02 software (Nikon Imaging Center at Northwestern University). Synaptic puncta were identified with a surface grain of 0.25 μm diameter because the puncta size in previously published data varied between 0.25 and 0.8 μm [10–12]. Parameters were set for both wavelength channels. Using IMARIS tools: surface rendering, fluorescence thresholding, and masking of unwanted immuno-labeling, we obtained the 3D structure of an individual pre-synaptic and post-synaptic puncta. Once the pre- and post-synaptic labeled surfaces were detected, the total number of pre-synaptic and post-synaptic surfaces was determined. Colocalization of pre- and postsynaptic surfaces ("synapse") was calculated with the XTension algorithm (Matthew Gastinger, 2015).

Inner hair cells on the above images were counted manually.

2.12. Counting of outer hair cells

The total number of outer hair cells at each frequency location (one microscopical field) was counted from confocal Z stacks imported into Fiji [13]. Outer hair cells/100 μm was calculated for each available sample image.

2.13. Statistics

Statistics, ANOVA and t-tests, were calculated with GraphPad Prism. Outliers in the raw data were identified by Rout and removed. For normal distributed data, an analysis of variance (ANOVA) was performed. Data with significantly different ANOVA were further analyzed with a TUKEY multiple comparison test. For the synapse data, the raw numbers were used in a mixed effect model (GraphPad Prism version 9.5.1), the Geisser-Greenhouse correction for sphericity, and a Tukey posttest. Significant statistical differences were concluded when $p < 0.05$.

3. Results

3.1. Fluvastatin protects against high level noise-induced hearing loss (NIHL)

Our prior work in guinea pigs indicated that fluvastatin delivered to one cochlea protected against NIHL in the contralateral cochlea (Richter et al., 2018). We saw in that study that the operated cochlea developed significant fibrosis in the scala tympani where the catheter is inserted, but that this fibrosis is not present in the contralateral side. Protection of ABR thresholds was less on the operated side than in the pristine, contralateral cochlea. In the present study, we were also concerned that the catheter inserted into the very small cochlea of the mouse would interfere with ABR measurements. Therefore, this work measures hearing only on the contralateral, unoperated side. Fig. 1 depicts the thresholds and threshold shifts in fluvastatin+noise treated animals at different times past the noise exposure.

As with the noise-alone graphs used to validate our physiology setup (Supplemental Fig. 2), fluvastatin + noise threshold shifts were stable by 1 week after noise exposure.

Fig. 2 limits the data to that measured 2 weeks after noise exposure (except for the unexposed, which, due to the unchanging thresholds, used the highest week measured after noise) and depicts the thresholds and threshold shifts at different frequencies.

Threshold shifts of the carrier +noise treated and the noise alone treated were similar. Average threshold shifts of the unexposed animals were less than 1 dB at all frequencies. Average threshold shifts (in dB) of fluvastatin+noise treated were lower than that treated with carrier + noise. Supplemental Table 1 lists the fluvastatin and carrier treatment measures' mean, standard deviation, and n, p at 4, 8, 12, 16, and 32 kHz. Statistics were carried out on the measures at 4, 8, 16, and 32 kHz. By ANOVA at each frequency (with Tukey multiple comparison test, noise and unexposed not shown), the differences between the fluvastatin treated and carrier were statistically significant (No statistics calculations were carried out at 12 kHz due to the small number of fluvastatin treated samples measured at that frequency).

These data indicate that fluvastatin delivered directly to the cochlea protects against NIHL in the contralateral cochlea as measured by the ABR thresholds and threshold shifts.

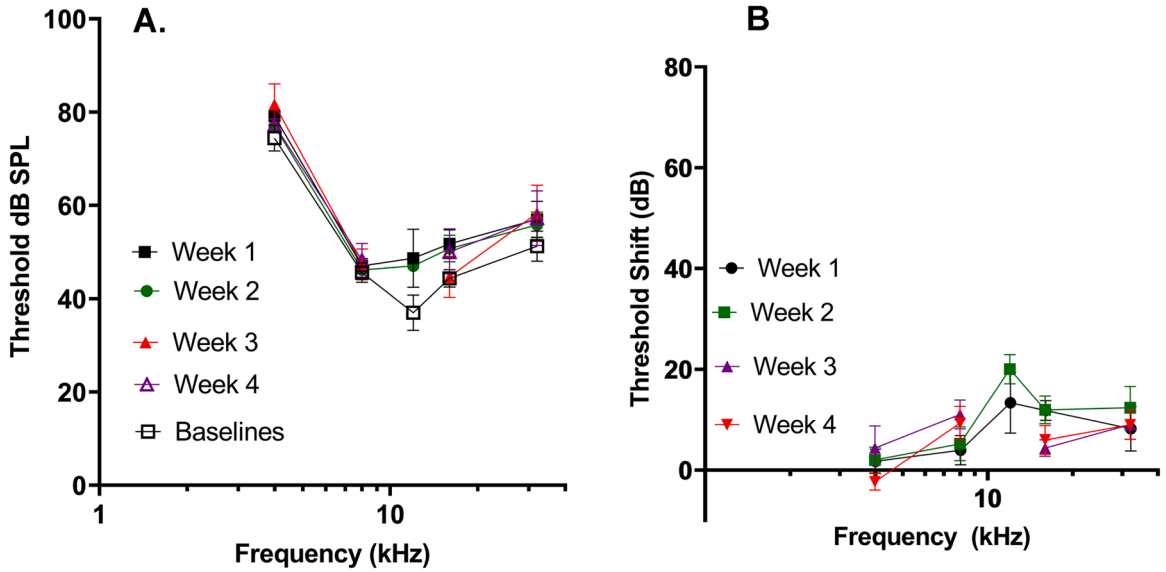

Fig. 1. Thresholds and threshold shifts after noise+fluvastatin 1–4 weeks after exposure to noise (110 dB SPL x 2 hr x 8–16 kHz). A) Thresholds do not change after 1 week. B). Calculated threshold shifts (the difference between threshold and individual baseline values) are below 20 dB and do not change after week 1. For all frequencies except 12 kHz: Week 1, n = 11; Week 2, n = 12; Week 3, n = 3; Week 4, n = 3. For 12 kHz Week 1 and 2, n = 3. There are no measures at 12 kHz for Weeks 3 and 4. Data show average ± SEM.

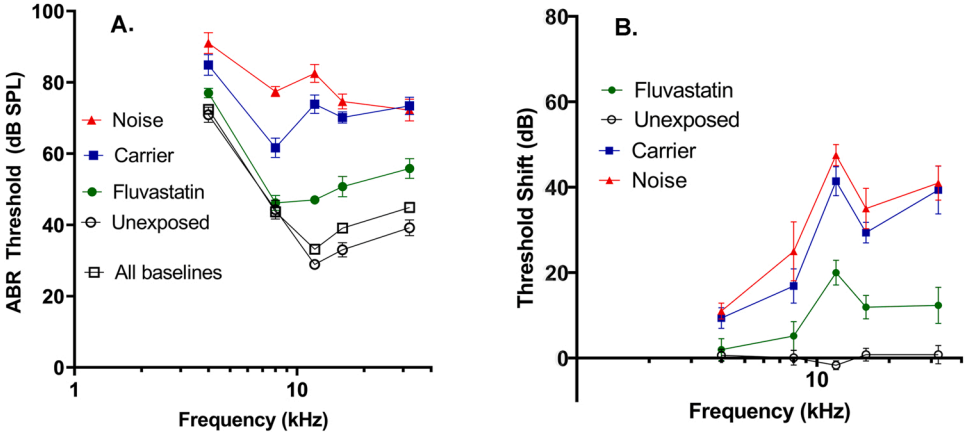

Fig. 2. Fluvastatin protects against noise induced hearing loss. A) ABR thresholds; B) Calculated threshold shifts (threshold minus individual baselines). Fluvastatin+noise, carrier+noise, and noise alone, two weeks after exposure to noise (110 dB SPL x 2 hr x 8–16 kHz). Unexposed animals were measured at week euthanized (equivalent to 1–4 weeks after noise exposure). Baselines were measured before the start of the experiment. Threshold shifts of the noise or carrier+noise treated mice were similar. Threshold shifts of unexposed mice did not vary more than 1 dB. Noise exposure+fluvastatin mice had smaller threshold shifts than those with noise or carrier+noise. Bars represent ± SEM. Supplemental Table I shows means ± SD and p values.

3.2. Cochlear structure

3.2.1. Inner hair cell synapses

Examples of inner hair cells with pre- and postsynaptic immunohistochemical labeling at the 16 kHz place are shown in Fig. 3. Each image depicts a partial microscopical field. Because the pre and post synaptic puncta and colocalization are automatically counted based on intensity, size and proximity, these images are not evaluated by eye, only by the software. A closer look at the pre, post and synaptic puncta is depicted in Supplemental Fig. 3.

Because the mice were not all carried for the same number of weeks after noise exposure, and thus were euthanized at different times, the sample sizes were small at each frequency for each time point. We limited our comparative statistics to synapse counts at two weeks for all groups except unexposed, which were counted at the time of euthanasia (equivalent to 1–4 weeks after noise exposure).

Fig. 4 shows the results of a mixed effects model of synapse counts at two weeks after noise (except for unexposed, which was as described). No statistical difference is observed between carrier and Fluvastatin at any frequency. The main differences are at 22 and 32 kHz. Both carrier and fluvastatin show statistical differences from the unexposed group. Even at 16 kHz, the average synapse/IHC between the carrier and fluvastatin is a little over 1. There is nothing known in the literature about the physiologic consequences of such a small change in synapse number. Overall, there is nothing in our synapse analysis to indicate that fluvastatin protects against noise induced synapses loss at the frequencies we are measuring. At 16 kHz, some individual points are identified by color filling and correlate with the indicated image in Supplemental Figure 3. Supplemental Table 2 shows the Average Synapses/inner hair cells, n and SD for each frequency.

In addition to our images and statistics, it was possible to visually compare our data with that in the literature (Fig. 5) [14]. The synapse counts in the published work by Fernandez et al. [14] were acquired from mice two weeks after exposure to 112 dB SPL x 2 h x 8–16 kHz, similar to our conditions (estimated using GetData Graph Digitizer 2.26 (S. Federov). These were expressed as percent of synapses in unexposed cochleas. When we expressed our fluvastatin data in a similar way in Fig. 5, we show that the average percent of surviving synapses per IHC ± SEM in the fluvastatin + noise group was similar to the published numbers for mice that were exposed to noise alone.

With this and the data below on inner hair cells and outer hair cells, we show that our work is consistent with that in the literature. These

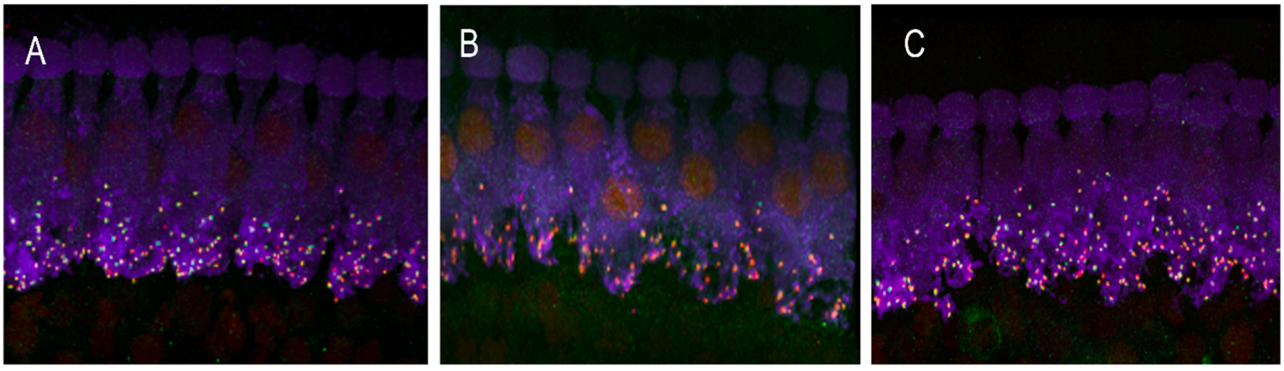

Fig. 3. Examples of immunolabeling of inner hair cells and synapses at the 16 kHz place. A) Unexposed; B) Carrier+ noise; C) Fluvastatin + noise. Purple, Myosin VII, Inner hair cells; Red, CtBP2, synaptic ribbons and also inner hair cell nuclei; Green; GluA2, post synaptic. Software uses intensity on each image, size and proximity of pre- and post- synaptic puncta to identify and count synapses. Supplemental Fig. 3 gives examples of labeling in the synaptic region of IHC from different cochleas.

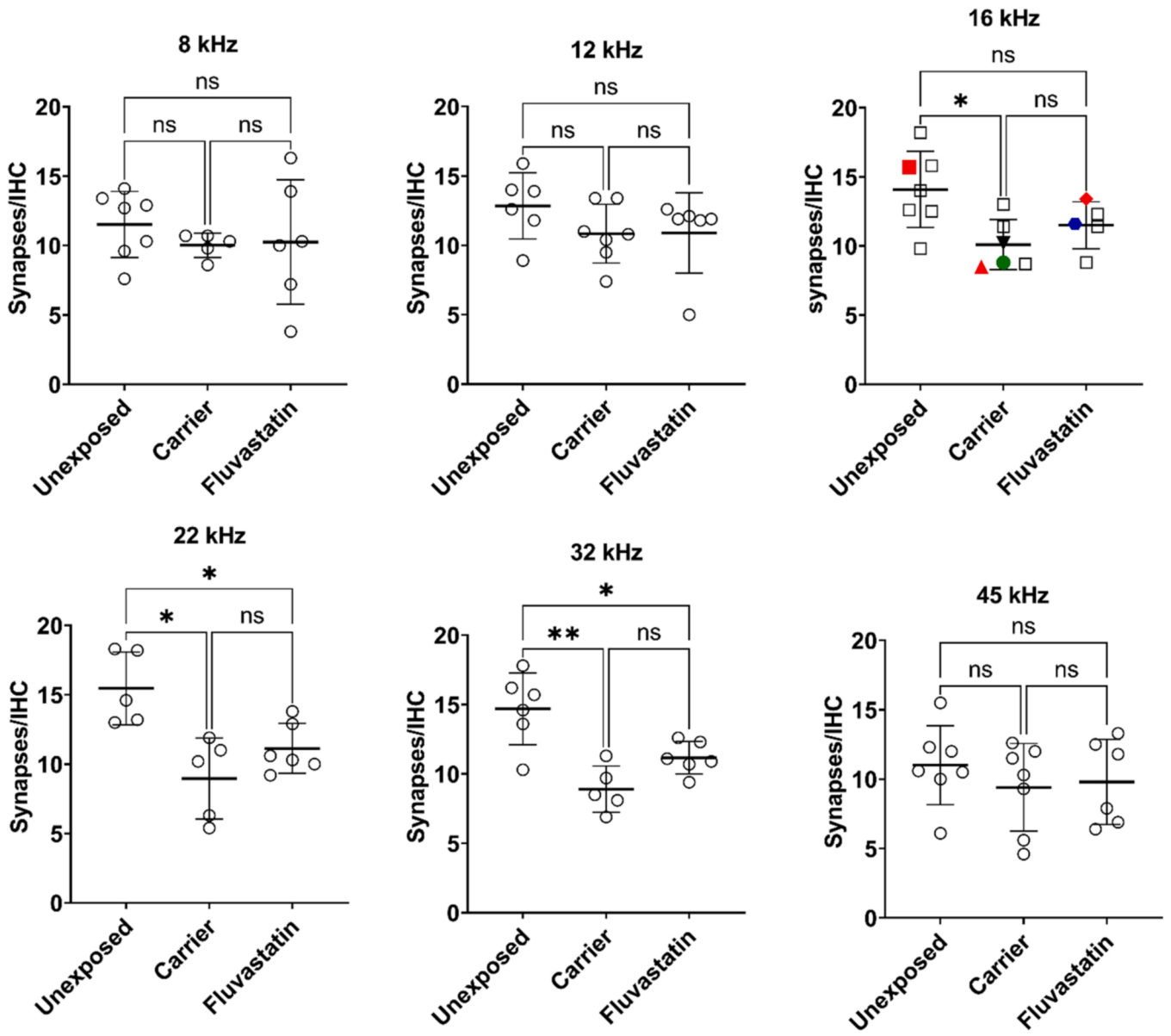

Fig. 4. Synapses/IHC at different frequencies in unexposed animals and animals treated with noise+carrier (2 weeks after noise) and noise+fluvastatin (two weeks after noise). Average ± . SD. At 16 kHz, the filled symbols correspond to the fields represented by the images in Supplemental Fig. 3. Unexposed - Red square, fields A-C; Carrier -Animal 1, red triangle, fields D-F; Carrier Animal 2, green circle, fields G-I; Carrier Animal 3, blue upside-down triangle, fields J-L; Fluvastatin Animal 1, red diamond, fields M-O; fluvastatin, Animal 2, blue hexagon, fields P-R. Values of p were calculated by mixed effects analysis (Graphpad) using Geisser-Greenhouse correction for sphericity, and correcting for multiple comparisons with Tukey. By this analysis, fluvastatin does not protect survival of inner hair cell synapses.

data support the hypothesis that although fluvastatin protected against 110 dB SPL x 2 hrs x 8–16 kHz noise-induced threshold shift, the protection does not appear to be associated with the protection of inner hair cell synapse survival at these frequencies.

3.2.2. *Hair cells*

Inner hair cells: Using the same tissue as used for synapses, we counted IHC at each frequency (Fig. 6; Supplemental Table 3). The survival of IHC was similar between the noise+carrier, noise-+fluvastatin and unexposed cochleas at any measured frequency. This is consistent with that in the literature showing retention of IHC at these frequencies after noise. Any differences between groups in our data would be very small and likely physiologically insignificant. It is known that a large proportion of IHC must be lost before there is an elevation of hearing threshold.

Outer hair cells: We counted outer hair cells (Fig. 7, Supplemental Table 4) in available tissue.

Unexposed cochleas were counted at the time of euthanasia (1–4 weeks after noise exposure of the other groups). Carrier +noise and fluvastatin + noise were counted at week 2 after noise exposure. OHCs/100 μm were counted up to the 45 kHz place, the highest frequency region counted, but only one fluvastatin treated cochlea was available at this frequency. Although the n is small at each frequency, these results are consistent with the Fernandez et al. study [14], showing little change in OHC counts after noise exposure up to 32 kHz, with only small differences at 45 kHz.

3.3. *Oral lovastatin*

The above experiments demonstrated that fluvastatin delivered to a local site behind the blood labyrinth border protects against NIHL. To examine whether an oral statin could also protect the cochlea from

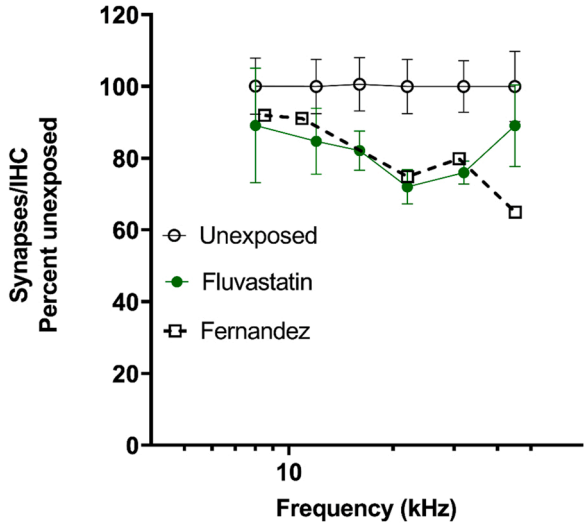

Fig. 5. Synapses/inner hair cell expressed as % of synapses in the unexposed control at each frequency (8–45 kHz). Fluvastatin+noise (110 dB SPL x 2 hr x 8–16 kHz), counted at two weeks after exposure to noise is compared to the data from Fernandez et al. [14] exposed to noise (112 dB SPL x 8–16 kHz x 2 h), also counted two weeks after exposure. Bars represent SEM. In this study, different numbers of animals were counted in each condition and at each frequency, as can be seen in Fig. 4. Fernandez et al. data, n = 10. Fluvastatin +noise showed similar decreases in percent synapses as that reported for noise alone by Fernandez et al. [14].

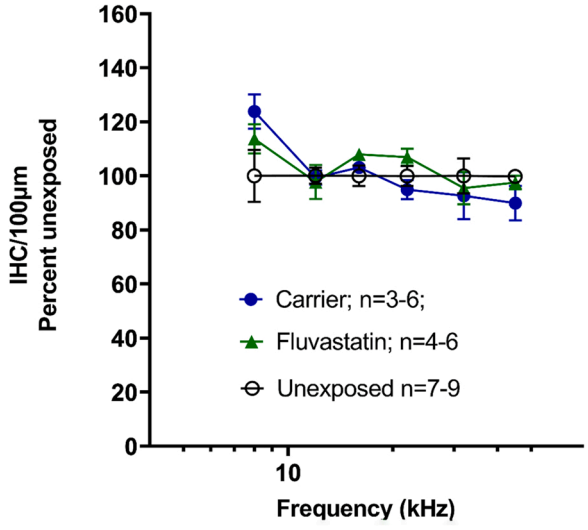

Fig. 6. Comparison of Inner hair cell (IHC) counts between carrier+ noise, fluvastatin+noise and unexposed mice (percent IHC in unexposed at each frequency). Carrier and fluvastatin measured at 2 weeks after noise exposure. Unexposed mice measured at age of euthanasia (1–4 weeks after the time of noise exposure in the other groups). The numbers of samples at each frequency for each condition were different. n = the range of animal numbers per frequency for each condition. Bars represent SEM. IHC numbers are similar between groups. See Supplemental Table 3 for actual n, SD for each frequency.

NIHL, we chose lovastatin, another HMG-CoA reductase inhibitor, because it had recently been demonstrated to preserve hearing in animals treated with cisplatin [15].

Fig. 8 shows results from the combined experiments using 60 mg/kg or 120 mg/kg. Thresholds were measured at baseline and week 2.

As expected, the carrier +noise treatment showed an elevation in threshold by about 45 dB at 12, 16, and 32 kHz. Animals that received lovastatin + noise showed smaller threshold shifts than the animals that only received the carrier. Differences were at least 20 dB between the two groups at each frequency tested.

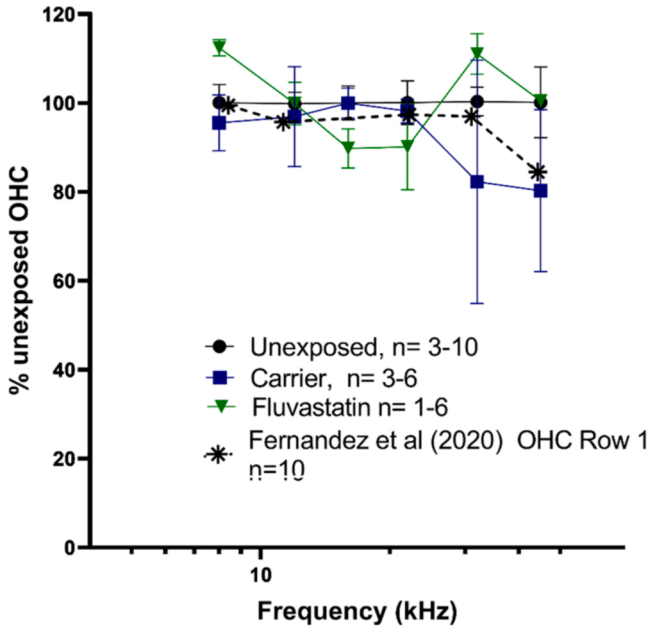

Fig. 7. Outer hair cells (percent of the average of OHC in unexposed mice at each frequency). Carrier+noise, fluvastatin + noise and unexposed. Fluvastatin and carrier counted at two weeks after noise exposure. Unexposed mice counted at time of euthanasia (1–4 week). n = range of numbers of mice measured per frequency. Average ± SEM. OHC numbers are similar to each other up to 32 kHz. (At 45 dB, only one fluvastatin mouse was available for counting). See Supplemental Table 4 for n, SD and average at each frequency.

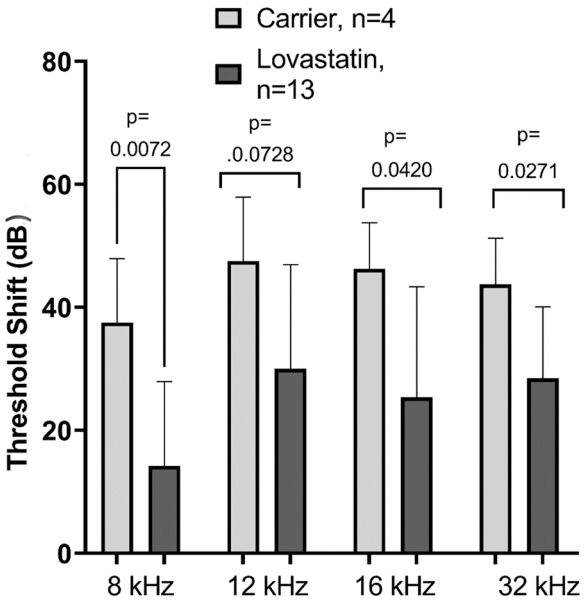

Fig. 8. ABR threshold shifts two weeks after noise in carrier+noise or lovastatin+noise exposed animals. Lovastatin given by gavage. Groups treated with 60 mg/kg and 120 mg/kg are combined in the graph. Bars indicate SD. Carrier+noise showed elevated threshold between about 40 and 50 dB, depending on frequency. Lovastatin+noise showed smaller elevations of between 10 and 30 dB, depending on frequency. By two- sided t-test, the differences between carrier and lovastatin are statistically significant at 8,16 and 32 kHz, and does not quite reach significance at 12 kHz. The data indicates that oral lovastatin can protect mice from noise induced hearing loss.

4. Discussion

Here we demonstrated that in CBA/CaJ mice, statins protect against ABR threshold elevation due to exposure to high level noise. We showed protection with two different delivery methods: fluvastatin delivered directly to the cochlear duct and lovastatin dosed orally. These data confirm that fluvastatin protects against NIHL in two different mammalian species. In addition, we improved the method for creating a cochleostomy in the mouse cochlea using a laser to assist surgery. This is the first time a surgical laser was used for this purpose in the mouse, and it saved time under anesthesia and created smaller and more consistent diameter holes in the cochlea.

In the fluvastatin-treated mice, we evaluated hair cell and synapse numbers at frequencies up to 45 kHz. The results were consistent with reports in the literature [14] showing that in mice, high-decibel noise alone produces no change in OHC numbers to 32 kHz and about a 20% reduction in inner hair cell synapses above 16 kHz. The decreases in synapses were not prevented by treatment with fluvastatin.

In our prior study in guinea pigs [3], we showed a loss of hair cells after high level noise exposure (120 dB SPL x 4 hr x 4–8 kHz) that was not seen in noise-exposed guinea pigs treated with fluvastatin. In this mouse study, the outer hair cells do not appear to degenerate with or without fluvastatin. However, hair cell function depends on more than cell survival. In the Fernandez et al. study [14], with 2-hour noise exposure similar to this study (112 dB x 2 hr x 8–16 kHz), DPOAE threshold shifts were elevated permanently above 16 kHz and as much as 35 dB at 32 kHz, suggesting abnormal function of the cochlea, due most likely to OHC functional deficit, but can be due to other causes of non-linearity of the basilar membrane. Cisplatin in mice was suggested also to impair OHC function as measured by DPOAE amplitudes. Oral lovastatin was reported to offer modest protection [15]. In our study of fluvastatin after high-level noise, surviving outer hair cell function could have been impaired but protected by fluvastatin, a possibility that needs further research.

An intriguing aspect of these fluvastatin studies is that the drug delivered directly into one cochlea protects against hearing loss in the contralateral cochlea, as we reported for guinea pigs [3]. At present, the mechanism of this protection is unknown. A handful of published reports indicate contralateral spreading of substances from one cochlea to the other either from intratympanic injection (particles [16], gentamicin [17]), or cochleostomy (viruses) [18]; fluvastatin [3]). These indicate that under favorable conditions – for example, delivery of a substance under pressure – substances can be transferred, and effects can be induced in the contralateral cochlea. The observation is so rare that in studies of auditory function, the contralateral cochlea is often used as a negative control, which we could not do in these experiments. The mechanistic possibilities for transfer range from transfer of the drug through the cerebrospinal fluid through the cochlear aqueduct [18]; transfer through the serum; or biochemical effects on neurons in the cochlea or brain that affect the contralateral cochlea. The actual mechanism of spreading an effect from one cochlea to the other could have implications for drug discovery and drug delivery to the inner ear.

Biochemically, statins have both cholesterol and non-cholesterol effects that could form the basis for hearing protection. First is the well-known inhibition of HMG-CoA reductase that results in the inhibition of cholesterol synthesis. Whether or not this affects the protection of hearing would depend on the turnover rates of cholesterol within the cochlear cells and in the blood vessels, since the effect of fluvastatin on hearing in the mouse is stable by 1 week after noise exposure and is maintained for at least 4 weeks. Alternatively, the HMG-CoA reductase pathway has multiple arms, and most do not involve cholesterol. Blocking the rate limiting enzyme in this pathway with a statin not only interferes with cholesterol synthesis but also has the potential to affect the synthesis of proteins and other molecules that depend on two downstream products of the pathway [19] – farnesyl-pyrophosphate (FPP) and geranylgeranyl-pyrophosphate (GGPP). FPP is a 15-carbon isoprenoid group, and GGPP is a 20-carbon isoprenoid group that is added to various substrates post-translationally – a reaction called prenylation. The hydrophobicity of these isoprenoid groups on proteins aids in trafficking to various membrane sites within the cells, affecting protein activity and function. Signaling molecules such as members of the Rho family are prenylated. If this prenylation is inhibited, the signaling molecules show altered activity and thus can affect the function and location of the enzymes and their effects on cytoskeleton, mitochondrial function, and intracellular and synaptic vesicles. Statins have also been shown to be able to alter gene expression and to modulate antioxidant and anti-inflammatory mechanisms, also altered by noise exposure, all of which are known to change after exposure to noise.

For this study and the guinea pig study, we chose to deliver fluvastatin directly to the cochlea to avoid the complication that the drug must, but cannot, cross the blood-labyrinth barrier. Oral dosing is a clinically relevant alternative that would not require any invasive methodology. It is not known, however, whether any of the seven statins currently in use would be able to pass the blood-labyrinth barrier or even if that is necessary for protective effects. Although the structures differ, it is nonetheless encouraging that at least some of the statins are known to pass the blood-brain barrier.

Reported studies of statins and hearing in inbred mouse models are few but increasing [19]. The few reports are varied in their approaches, hearing insults, and methods. Still, they do show at least some protection against hearing loss caused by cisplatin [15], broadband noise [20], hyperlipidemia [21], and antibiotic treatment [22,23].

Although the mechanisms by which statins protect hearing is presently unknown, the availability of a statin responsive mouse model with limited variation in NIHL will allow in depth studies of the biochemical and genetic mechanisms mediating statin protection and may shed light on additional methods of drug delivery and optimization.

NIHL affects 26 million people in the USA between the ages of 20 and 69. Hearing protection by a widely available, affordable statin is potentially important and could impact the millions of hearing-impaired worldwide.

Funding

This work was supported by the Department of the Navy, Office of Naval Research, grants #N00014182508; N00014512130; and the Office of the Assistant Secretary of Defense for Health Affairs through the Hearing Restoration Research Program under Award no W81XWH-20-1-0484.

CRediT authorship contribution statement

Frédéric Dépreux: Data curation, Formal analysis, Investigation, Writing – original draft, Writing – review & editing. **Lyubov Czech:** Data curation, Formal analysis, Investigation, Methodology, Writing – review & editing. **Hunter Young:** Investigation, Writing – review & editing. **Claus-Peter Richter:** Investigation, Methodology, Resources, Software, Writing – review & editing. **Yingjie Zhou:** Methodology. **Donna S. Whitlon:** Conceptualization, Formal analysis, Funding acquisition, Project administration, Supervision, Validation, Visualization, Writing – original draft.

Declaration of Competing Interest

The authors declare the following financial interests/personal relationships which may be considered as potential competing interests: Donna Whitlon and Claus-Peter Richter are inventors on patents #9.150.533 and #9.517.233 issued to Northwestern University.

Acknowledgements

Special thanks to Constadina Arvanitis, Ph.D. and David

Kirchenbuechler, Ph.D from Northwestern University Center for Advanced Microscopy generously supported by NCI CCSG P30 CA060553 awarded to the Robert H Lurie Comprehensive Cancer Center.

Appendix A. Supporting information

Supplementary data associated with this article can be found in the online version at doi:10.1016/j.biopha.2023.114674.

References

[1] D.S. Whitlon, Drug discovery for hearing loss: Phenotypic screening of chemical compounds on primary cultures of the spiral ganglion, Hear Res 349. doi: 10.1016/j.heares.2016.07.019.
[2] D.S. Whitlon, M. Grover, S. Dunne, S. Richter, C.-H. Luan, C.-P. Richter, Novel high content screen detects compounds that promote neurite regeneration from cochlear spiral ganglion neurons, Sci. Rep. 5 (2015) 15960, https://doi.org/10.1038/srep15960.
[3] C.P. Richter, H. Young, S.V. Richter, V. Smith-Bronstein, S.R. Stock, X. Xiao, C. Soriano, D.S. Whitlon, Fluvastatin protects cochleae from damage by high-level noise, Sci. Rep. 8 (1) (2018) 3033, https://doi.org/10.1038/s41598-018-21336-7.
[4] A.E. Luebke, P.K. Foster, Variation in inter-animal susceptibility to noise damage is associated with alpha9 acetylcholine receptor subunit expression level, J. Neurosci. 22 (10) (2002) 4241–4247, https://doi.org/10.1523/JNEUROSCI.22-10-04241.2002.
[5] Y. Wang, K. Hirose, M.C. Liberman, Dynamics of noise-induced cellular injury and repair in the mouse cochlea, J. Assoc. Res Otolaryngol. 3 (3) (2002) 248–268, https://doi.org/10.1007/s101620020028.
[6] C. National Research Council Committee for the Update of the Guide for the Care and Use of Laboratory Animals, eighth ed., National Academies Press (US), 2011 https://doi.org/10.17226/12910.
[7] S.C. Montgomery, B.C. Cox, Whole mount dissection and immunofluorescence of the adult mouse cochlea, J. Vis. Exp.: JoVE 107 (2016), https://doi.org/10.3791/53561.
[8] T.T. Hickman, K. Hashimoto, L.D. Liberman, M.C. Liberman, Cochlear synaptic degeneration and regeneration after noise: effects of age and neuronal subgroup, Front Cell Neurosci. 15 (2021), 684706, https://doi.org/10.3389/fncel.2021.684706.
[9] L.D. Liberman, J. Suzuki, M.C. Liberman, Dynamics of cochlear synaptopathy after acoustic overexposure, J. Assoc. Res Otolaryngol. 16 (2) (2015) 205–219, https://doi.org/10.1007/s10162-015-0510-3.
[10] X. Chen, C. Winters, R. Azzam, X. Li, J.A. Galbraith, R.D. Leapman, T.S. Reese, Organization of the core structure of the postsynaptic density, Proc. Natl. Acad. Sci. USA 105 (11) (2008) 4453–4458, https://doi.org/10.1073/pnas.0800897105.
[11] M. Sheng, E. Kim, The postsynaptic organization of synapses, Cold Spring Harb. Perspect. Biol. 3 (12) (2011), https://doi.org/10.1101/cshperspect.a005678.
[12] D. Dumitriu, S.I. Berger, C. Hamo, Y. Hara, M. Bailey, A. Hamo, Y.S. Grossman, W. G. Janssen, J.H. Morrison, Vamping: stereology-based automated quantification of fluorescent puncta size and density, J. Neurosci. Methods 209 (1) (2012) 97–105, https://doi.org/10.1016/j.jneumeth.2012.05.031.
[13] M. Abramoff, S. Magalhaes, S. Ram, Image processing with ImageJ, Biophotonics Int. 11 (7) (2004) 36–42.
[14] K.A. Fernandez, D. Guo, S. Micucci, V. De Gruttola, M.C. Liberman, S.G. Kujawa, Noise-induced cochlear synaptopathy with and without sensory cell loss, Neuroscience 427 (2020) 43–57, https://doi.org/10.1016/j.neuroscience.2019.11.051.
[15] K.A. Fernandez, K.K. Spielbauer, A. Rusheen, L. Wang, T.G. Baker, S. Eyles, L. L. Cunningham, Lovastatin protects against cisplatin-induced hearing loss in mice, Hear. Res. 389 (2020), 107905, https://doi.org/10.1016/j.heares.2020.107905.
[16] S.Y. Lee, J. Kim, S. Oh, G. Jung, K.J. Jeong, V. Tan Tran, D. Hwang, S. Kim, J. J. Song, M.W. Suh, J. Lee, J.W. Koo, Contralateral spreading of substances following intratympanic nanoparticle-conjugated gentamicin injection in a rat model, Sci. Rep. 10 (1) (2020) 18636, https://doi.org/10.1038/s41598-020-75725-y.
[17] P. Roehm, M. Hoffer, C.D. Balaban, Gentamicin uptake in the chinchilla inner ear, Hear Res 230(1-2) ((2007) 43–52, https://doi.org/10.1016/j.heares.2007.04.005.
[18] T. Stöver, M. Yagi, Y. Raphael, Transduction of the contralateral ear after adenovirus-mediated cochlear gene transfer, Gene Ther. 7 (5) (2000) 377–383, https://doi.org/10.1038/sj.gt.3301108.
[19] D.S. Whitlon, Statins and hearing, Hear Res (2022), 108453, https://doi.org/10.1016/j.heares.2022.108453.
[20] J. Park, S. Kim, K. Park, Y. Choung, I. Jou, S. Park, Pravastatin attenuates noise-induced cochlear injury in mice, Neuroscience 208 (2012) 123–132, https://doi.org/10.1016/j.neuroscience.2012.02.010.
[21] Y.Y. Lee, O.-s Choo, J.K. Kim, E.S. Gil, J.H. Jang, Y. Kang, Y.-H. Choung, Atorvastatin prevents hearing impairment in the presence of hyperlipidemia, BBA Mol. Cell Res. 1867 (2020), 118850, https://doi.org/10.1016/j.bbamcr.2020.118850.
[22] Y. Wu, W. Meng, M. Guan, X. Zhao, C. Zhang, Q. Fang, Y. Zhang, Z. Sun, M. Cai, D. Huang, X. Yang, Y. Yu, Y. Cui, S. He, R. Chai, Pitavastatin protects against neomycin-induced ototoxicity through inhibition of endoplasmic reticulum stress, Front. Mol. Neurosci. 15 (2022), 963083, https://doi.org/10.3389/fnmol.2022.963083.
[23] C.H. Lee, J. Jeon, S.M. Lee, S.Y. Kim, Pravastatin administration alleviates kanamycin-induced cochlear injury and hearing loss, Int. J. Mol. Sci. 23 (9) (2022), https://doi.org/10.3390/ijms23094524.

ALZET pump implantation in mice for chronic drug delivery

Frederic Depreux
Northwestern University Feinberg School of Medicine
Donna Whitlon
Northwestern University Feinberg School of Medicine
Claus-Peter Richter (cri529@northwestern.edu)
Northwestern University Feinberg School of Medicine

Method Article

Keywords: Mouse, surgery, cochleostomy, bullostomy, chronic implantation, micro-osmotic pump, drug delivery

Posted Date: July 5th, 2023

DOI: https://doi.org/10.21203/rs.3.rs-3135966/v1

Abstract

Drugs, chemical compounds, and other elements are often delivered to the ear of experimental animals to manipulate cochlear function, study how the ear works, identify drugs that prevent hearing loss, and test for ototoxicity. Delivery procedures for acute studies have been described in the literature. However, detailed information on methods that allow weeks of continuous drug delivery to mice cochleae is sparse. This paper describes a method for chronic drug delivery to the mouse cochlea. We illustrate the steps for the surgical implantation of an ALZET infusion pump and the placement of its catheter. We propose a ventral approach to the cochlea, using a surgical laser to make the cochleostomy and the placement of the pumps' delivery ports into scala tympani or scala vestibuli. Depending on the experimental questions to be tested, the catheter can be directed toward the cochlear base, the vestibular system, or the cochlear apex.

1. Introduction

Drugs and chemical compounds are often delivered to the cochlea of experimental animals to study normal function, ototoxicity, and the potential to treat noise-induced hearing loss. Several research groups have presented methods for direct cochlear drug delivery[1,2]. The published techniques include transtympanic drug injection into the middle ear[3-9], sponges or gels placed on the round window[10-13], microinjection through the round window[14], nano-carriers[15-18], and direct delivery of drugs with pumps into the cochlea[14,19-23]. Recently, Kim and Ricci surgically exposed mouse cochleae and applied phosphoric acid gel to create a window in the cochlear wall that permits the imaging of cochlear cells in hearing animals[24]. Among the methods, direct drug injection into scala tympani provides a well-controllable approach for cochlear drug delivery[14,22,25-32]. While previous papers describe the technique of implanting an osmotic pump to deliver the chemical components[21,22], careful evaluation of the published methods shows that only in larger animals, such as gerbils or guinea pigs, implanted osmotic pumps delivered drugs for weeks. Only a few publications are available on intracochlear drug delivery in mice[14,33]. Examples are Chen and coworkers, who delivered the drugs for less than three hours[33]. Jero and coworkers compared different methods for drug delivery to the inner ear. They showed that transtympanic injection, sponges placed on the round window, and direct cochlear injection with an osmotic pump could deliver the drugs. In their short term, approximately 72 hours of experiments, the mice recovered from anesthesia[14].

To deliver drugs for up to four weeks directly into the mouse cochlea, we implanted an ALZET® micro-osmotic pump. The surgery is a modification of the approach reported by Jero et al. (2001) but uses a surgical carbon dioxide (CO_2) laser to make the bullostomy and the cochleostomy. The cochleostomy was rostral, as close as possible to the stapedial artery and the middle ear's medial wall. This approach also allowed us to select the placement of the pump catheter into scala vestibuli by moving the cochleostomy site toward the cochlear base. With the chosen cochlear access, the catheter orifice and

subsequent direction of the drug flow could be oriented either toward the cochlear base, including the vestibular system, or the cochlear apex.

2. Methods and Results

2.1 Ethical statement

The animal experiments described below complied with the ARRIVE (Animal Research: Reporting of In Vivo Experiments) guidelines. Care and use of the animals followed the NIH Guide for Care and Use of Laboratory Animals guidelines[34]. All procedures were approved by The Institutional Animal Care and Use Committee (IACUC) at Northwestern University (IS00008596 and IS00008707) and by the Navy Bureau of Medicine and Surgery (BUMED)

2.2 Animals

Ten-week-old CBA/CaJ male mice (stock number 000654) were shipped from Jackson Laboratory (Bar Harbor, ME) to the Center for Comparative Medicine at Northwestern University, Chicago. The mice were acclimated for two weeks in the facility before surgery. Three animals were housed together in an autoclaved, individually ventilated cage of 36 cm (L) x 18 cm (W) x 12 cm (H), having wood shavings and cotton pads for the nest and hiding place building. The light cycle was 14 hours, followed by 10 hours of dark. The lights were “on” at 6 am and “off” at 8 pm. Water and Teklad (Envigo, Indianapolis, IN) LM-485 Mouse/Rat sterilizable diet pellets were given *ad libitum*. Post-surgery, mice were individually housed to prevent chewing and scratching at the sutures.

2.3 Osmotic pump implantation

2.3.1 The catheter for the osmotic pump

The catheter inserted into the cochlea was custom fabricated to reduce the tubing diameter from 1 mm at the port of the osmotic pump to 130 µm, where it enters the cochlea. Supplemental Figure 1 shows the fabrication steps (Supplemental Table 1 lists the materials and sources). A 2 cm long segment of polyimide tubing (Micolumen, Oldsmar, FL), 130 µm outer and 100 µm inner diameter, was inserted into the Tygon® ND100-65 tubing (Saint Gobain Performance Plastic, Akron, OH), 840 µm inner diameter. The connection was sealed with SILASTIC® MDX4-4210 medical-grade elastomer mixed with its curing agent (Dow Corning, Midland, MI). The fabricated catheters were then placed in an oven for overnight polymerization to form the silicone rubber at 50°C (Supplemental Figure 1). Before sterilization by ethylene oxide gas exposure, the quality of each catheter was individually tested (Supplemental Figure 1). The catheter length was adjusted for proper pump placement when the pump and its catheter were used in the surgery.

2.3.2 Materials required and preparation of the surgery

Before the surgery, all instruments (Supplemental Figure 2 and Supplemental Table 2) were autoclaved. Catheters that connect the osmotic pump and the cochlea were sterilized using ethylene oxide gas (Supplemental Table 3). We also gathered the materials required for anesthesia (Supplemental Table 4) and collected the disposable and miscellaneous items (Supplemental Table 5) for the surgery.

2.3.3 The surgical team

A two-person team was optimal for the procedure; one person was trained in performing surgeries under aseptic conditions. The second, a support person, was responsible for inducing the anesthesia, mounting the mouse in the head holder, shaving, and cleaning the surgical field, keeping medical records, monitoring, and adjusting the anesthesia, and supervising the animal's recovery after surgery.

2.3.4 Animal anesthesia

For pain management, we injected a subcutaneous dose of 0.05 mg/kg immediate-release Buprenorphine analgesic[35,36] at least an hour before the induction of the anesthesia, followed thirty minutes later by an intraperitoneal injection of 1 mL of 0.9% NaCl United States Pharmacopeia (USP) solution for hydration. The anesthesia was induced with 3% of the inhalation anesthetic isoflurane in 0.3 L/min oxygen by placing the mouse into a commercially available induction box (23 cm (length) x 10 cm (width) x 10 cm (height)). The mouse was then transferred from the induction box to a water-based heating pad covered with a paper underpad and placed into a custom-made head holder. Isoflurane, 1-3% in 0.3 L/min oxygen, delivered via a nose cone, was used to maintain the level of anesthesia (Figure 1**(a)** and Supplemental Figure 3).

2.3.5 Preparation of the surgical field

With a commercially available Wahl clipper (Supplemental Table 2), the animal’s fur was removed well beyond the expected incision line (Figure 1**(a)**). The area was cleaned three times with betadine solution and 75% alcohol in alternate order, wiping the cleaning fluid away from the center of the surgical field. Drapes under the animal and drapes covering the nose cone and exposed animal parts created a sterile field. Towel Clamps (Supplemental Figure 2 and Supplemental Table 2: Tool #1) held the drapes in place.

2.3.6 Access to the bulla

Figure 1 shows in detail the surgical access to the bulla. First, in the supine position, the mouse is mounted to the nosecone of the custom-made head holder (Figure 1**(a)**). The surgery begins with an approximately 2 cm skin incision using a small pair of sharp scissors (Supplemental Table 2: Tools #2 and #3) starting close to the right shoulder, lateral from the midline, towards the mandible along the dashed white arrow (Figure 1**(a)**). Using blunt dissection, the tissue over the submandibular glands (SMGs) was removed (Figure 1**(b)**), and the anterior belly of the digastric muscle (AD) became visible. The white dashed line in Figure 1**(b)** highlights the boundary between the left and right SMG, along which they were separated (Figure 1**(c)**, Supplemental Table 2: Tool #2). Retracting the right SMG exposed the

entire digastric muscle with its anterior (AD) and posterior bellies (PD). The PD was the landmark to approach the bulla. The white arrow in Figure 1**(c)** points to the location of the bulla below the PD. Scissors were not used for the surgery's following steps to minimize the risk of cutting small blood vessels. Instead, the tissue was dissected carefully with sharp forceps (Supplemental Table 2: Tools #4 and #5) to expose the digastric muscle's origin. Figure **1(d)** shows the bulla after elevating the PD; the bulla and outer ear canal are visible (dashed box, Figure 1**(d)** and Supplemental Table 2: Tools #4 and #5). It is important not to manipulate the facial nerve (thick arrow). After the dissection, the muscles were retracted with a custom-made tool (Supplemental Figure 2**(c)**, Supplemental Table 2: Tool #6). Careful muscle dissection with pointed forceps exposed the bulla (Figure 2**(a)-(b)** and Supplemental Table 2: Tools #4 and #5).

2.3.7 Opening the bulla and creating the cochleostomy

The surgical bullostomy and cochleostomy are made using a sharpened pick, motorized drill with a burr, or a CO_2 laser. Any tools will work for the bullostomy (Figure 2(**c**)), but the cochleostomy is more challenging (Figure 2(**d**)-(**e**)-(**f**)). The burr and the pick often impede the cochlea's direct view, frequently resulting in a much larger cochleostomy than required to insert the osmotic pump's catheter. In contrast to the burr, the CO_2 laser allows adequate visual control over the cochleostomy site while creating the opening (Figure 2**(f)**). However, using the laser bears the risk of nicking the stapedial artery. To use the pick for making or enlarging the cochleostomy (Supplemental Figure 2 and Supplemental Table 2: Tool #7), the tip of the pick should be less than 100 µm in diameter.

2.3.8 ALZET® pump placement

Supplemental Figure 4 describes the intraoperative catheter and osmotic pump assembly, and Figure 3 the surgical placement. For the pump assembly, the catheter, the osmotic pump, and its access port were placed (Supplemental Figures 4**(a)**-**(b)** on the sterile drape. The ALZET® pump was loaded with the drug using the filling needle. The catheter was shortened (Supplemental Figure 4**(b)**) and connected to the access port (Supplemental Figure 4**(c)**). Before joining the catheter to the pump, it was flushed with the drug, ensuring no air bubbles had been introduced (Supplemental Figures 4**(d)**-**(e)**). The fluid drop at the catheter's tip (Supplemental Figure 4**(f)**) confirms the pump's successful assembly. The assembled ALZET® pump was inserted into a pocket under the skin over the thorax (Figure 3**(a)**), which was made by blunt dissection with a pair of pointed scissors. Two pairs of forceps (Supplemental Figure 2 and Supplemental Table 2; Tools #4 and #5) were used to manually insert the pump towards the shoulder blades and push it into its final position. Since the osmotic pump was placed on the animal's back, its catheter was positioned below the sternocleidomastoid muscle (Figures 3**(b)** and 3**(c)**). After tunneling the catheter, its tip was gently bent (Figures 3**(b)**-**(c)**) and inserted with a pair of fine forceps (Supplemental Figure 2 and Table 2; Tool #5) through the cochleostomy (Figure 3**(c)**). The cochleostomy was slightly larger than the catheter's outer diameter. Additional tissue was required to seal the opening.

The cochleostomy's exact location and the catheter orientation determined whether the catheter's orifice was toward scala tympani or scala vestibuli. Cochleostomy sites closer to the stapes and the catheter's orientation toward the cochlear base placed the tubing tip into scala vestibuli. In contrast, cochleostomy locations closer to the stapedial artery and the bulla's medial wall with catheter orientations toward the bulla's medial wall placed the catheter's tip into the scala tympani. In some experiments, we confirmed the catheter tips' locations through micro-computed tomography with synchrotron radiation (see the section below: Image acquisition and tomographic reconstruction, Figure 4**(a)**). After placing the catheter, we stabilized it in its position by filling the middle ear cavity with dental acrylic using a 1 mL syringe and 22G needle (Figure 3**(e)**). During the 5 minutes of acrylic polymerization, we covered the bulla with the SMG and skin to limit desiccation (Figure 3**(f)**).

2.3.9 Skin closure and suture

The skin incision was closed with two layers using interrupted sutures (Supplemental Figure 2 and Supplemental Table 2: Tool #8 or #11 and #9). For the first layer, we used 6-0 (VICRYL) absorbable suture material and 6-0 (ETHICON) non-resorbable suture for the skin. During this last step, the percentage of isoflurane was decreased to a minimum of 1-1.5% under continuous monitoring of the mouse's anesthesia level. The closed incisions were cleaned with two alternating swaps of Betadine solution and alcohol (75%). The anesthetic delivery was discontinued, and the animal was removed from the head holder and placed in the supine position in a recovery box on top of a heating pad. The animal was under continuous supervision until sternal and freely ambulant. The recovery time was, on average, 6 minutes (min) and 52 seconds (s) (2 – 19 min, n = 45) after stopping the flow of isoflurane (Figure 5). The pump was visible on the mouse's back but did not affect the animal's movements and activity (Figure 4B, Supplemental Video 1).

2.3.10 Post-surgical pain management

For post-surgical pain management, we injected Buprenex subcutaneously (SC) every 12 hours over 48 hours.

2.3.11 Post-surgical animal handling

Animal handling after the surgery was gentle to avoid dislocation and damage to the newly implanted osmotic pump. Mice were single-housed in fresh and clean cages after the surgery to prevent the risk of injury by cage mates. Some of the former cotton bedding/nest was transferred into a new cage to reduce mouse stress from being left alone in a new environment. A food paste made of water-saturated food pellets was placed in the cage close to the mouse nest for easy access. It was essential to change the food every day. Visual mouse pain monitoring included but was not limited to, looking for the shape of eyelids, porphyrin patches around the eyes, back positioning, the status of nest building, the animal's activity level, and gait during frequent mouse observations [37-41]. The animals' weight was monitored over two weeks.

2.4 Image acquisition and tomographic reconstruction

All cochleae were imaged at the 2-BM-B beamline of the Advanced Photon Source (APS) using monochromatic radiation with photon energies of 22 kilo-electron volts (keV). The detector-sample distance was 600 mm for phase contrast. A 5x objective lens was used in the detector system, resulting in an approximately 3x3 mm^2 field of view. Over a range of 180 degrees, we captured projections of each sample at increments of 0.12 degrees. The exposure time for a single image was 0.2-0.3 s. At the beginning and end of each image series, flat field images (no object in the beam path) were recorded; after the series, a dark field image (the radiation beam was blocked) was captured.

The projections were used to reconstruct the cochlea. Custom-written phase retrieval software for non-interferometric phase imaging with partially coherent X-rays was used[42-44]. Reconstructions were on a 2048 x 2048 grid with custom-written software[45]. The reconstructions resulted in 1.45 µm isotropic voxels. The spatial resolution was determined from the system's response to a sharp discontinuity in the image, such as a bony edge. The parameter measured was the distance required for the gray values to fall from 90% to 10%. The resulting distance was 4.4 µm.

2.5 Events observed during and after surgery

Under optimal anesthesia, the mouse's expected heart rate is between 300 to 450 beats per minute (bpm), with an oxygen saturation above 96% and a breathing rate of around 55-65 breaths/min[46]. Four out of 45 mice (8.9%) had an episode with fewer than 50 bpm breathing rates. Decreasing the isoflurane concentration to 0.5% for 1 to 3 minutes restored normal breathing and respiratory rates. While little to no bleeding during the surgeries is typical, in 6 out of 45 mice (13.3%), for example, bleeding from the jugular vein occurred after the retractor nicked the vessel. Gentle pressure with a sterile cotton-tipped applicator stopped the bleeding. Bleeding also occurred while making the cochleostomy (3 mice, 6.7%). Since the mouse's head was not tightly fixed in the head holder, it moved slightly from the animal's breathing. The stapedial artery moved similarly, and in rare instances, into the beam path of the CO_2 laser or drilling while creating the cochleostomy. Bleeding by opening the stapedial artery could be severe, and it was difficult to stop. It is important to record bleeding events and episodes of hypoxia as they may affect mouse hearing.

The vestibular system is close to the cochlear base and can be affected by the catheter's placement. Symptoms indicating vestibular stimulation or damage (VDs) included a tilted head, shaking the head, a twirling body, and the mouse's inability to extend arms toward the cage to grab it while held by the tail. Vestibular symptoms showed in 19 out of 45 mice up to 72 hours post-surgery and did not recover over time. All mice showing vestibular symptoms had the catheter implanted toward the base of the cochlea.

Overall surgical and recovery times were not affected by the above-described incidents (Figure 5). After surgery, the mice's body weight decreased by 3.56 ± 3.12% and 6.28 ± 9.90% at 24 hours and one week, respectively. The body weight was back or above pre-surgery two weeks after the surgery. On average,

mice presenting signs of vestibular damage lost more weight (11.95 ± 12.73% one-week post-surgery). Two mice from the VD group were euthanized for losing more than 25% of body weight during the first week after the surgery (Supplemental Figure 5). No other animal required euthanasia in this study.

3. Discussion

A modified ventral approach to the cochlea allows the implantation of an osmotic pump for long-term drug delivery in mice. Our modifications to the published procedure[14,33] include different locations for the bullostomy and cochleostomy and the use of a laser. The manuscript provides a detailed description of the ALZET® mini-osmotic pump implantation and the surgical outcomes. In contrast to the dorsal approach described for electrode placement[47], labyrinthectomy, and vestibular neurectomy[48], the ventral approach provides easier access to the cochlea with the mouse fixed on the nasal holder. It offers better control over the facial nerve, as Jero et al. discussed[14]. The ventral approach also offers minimal morbidity and mortality.

Our protocol stresses the approach to the middle ear by using the digastric muscle as a landmark. Identifying the posterior digastric muscle allows for moving quickly to the ear with minimal displacement of adjunct tissues. The use of a small retractor maintains the field of view. At the conclusion of the surgery, skin closure in two layers reduces the risk of wound dehiscence.

Mice are social animals, and single housing after surgery may delay recovery [49]. However, the single housing of the surgically treated mice is important. Housed together, they tend to chew their sutures resulting in wound dehiscence.

To deliver drugs immediately after implantation, Alzet osmotic pumps require several hours of priming in sterile saline solution at 37°C. The priming time depends on the model (https://www.alzet.com/resources/alzet-technical-tips/#1560367975183-ba1896c5-0e75/). Based on experimental consideration, this step can be omitted to circumvent any break in the sterile chain of the pump.

Hemorrhage and reduced respiratory rate episodes were the two surgical events that required quick intervention. However, surgery length, sternal recovery time, and body weight were not different in mice with complications from mice exhibiting no surgical problems (“fine” group). The stapedial artery, persistent in adult mice [50], is a branch of the internal carotid artery. The stapedial artery passes through the stapes, branches of the medial meningeal artery, and runs rostrally, forming its infraorbital branch. The stapedial artery does not constitute a blood supply for the cochlea and has been obliterated during surgical approaches[51] without affecting cochlear function. Consequently, bleeding from the stapedial artery unlikely affects the cochlea but causes problems through blood accumulation in the middle ear. Injuring the jugular vein with the retractor was less severe. The primary bleeding issue may relate to decreased total blood volume. Both respiratory distress and severe bleeding during the surgery resulted in elevated ABR thresholds in our hands. Even if post-surgical recovery of animals encountering noticeable

bleeding during surgery did not seem to differ from the “fine” group, study rigor might require excluding these animals.

The typical isoflurane setting was 1-1.5% after the anesthesia induction. Settings must deliver enough anesthetic to ensure a sufficient anesthesia level but not expose the mice to excessive isoflurane, depressing breathing, and increasing anesthesia recovery times. Isoflurane is a non-flammable volatile anesthetic approved by the Federal Drug Administration for general anesthesia induction and maintenance in humans and animals[52]. According to Constantinides et al.[53], isoflurane is the primary anesthetic used in mouse animal models. In the central nervous system, isoflurane likely inhibits neurotransmitter-gated ion channels such as GABA, glycine, and NMDA receptors[52,54]. Skeletal muscles, including thorax ones, become relaxed, increasing $PaCO_2$[52]. Therefore, inadequate high isoflurane levels lead to bradycardia and lower respiratory rates[46]. Episodes of reduced respiratory rates during a few surgeries may have originated from too deep anesthesia levels.

Similar to Jero et al.[14], we observed vestibular symptoms in implanted mice. The direction of the catheter toward the cochlear base correlates with the frequency of vestibular symptoms. Vestibular symptoms, such as those described in the 2.2.13 section, may result from mechanical damage caused by advancing the catheter too far towards the cochlear base or through the direct flow of the injected fluids into the cochlea. Vestibular function was not systematically assessed by measuring vestibular myogenic or sensory evoked potentials (VEMP or VsEP)[55-61]. Therefore, the number of mice with post-surgical vestibular deficiencies may underestimate the number of mice affected. It is essential to realize that vestibular damage, especially if severe, is debilitating for the mouse. It is likely disrupting the affected mouse's ability to feed and drink adequately, particularly during the critical surgical recovery period. Mice may lose excess weight, so they must be euthanized or removed from the study.

Placement of the catheter toward the base in the scala tympani[22] likely delivers drugs near the cochlear aqueduct[62]. Diffusion of the drug to the contralateral ear[22,63-65] might be possible.

Declarations

Acknowledgments

This work was supported by grants from the Office of Naval Research (N000141210173; N000141512130; N000141612508); a grant from the Office of the Assistant Secretary of Defense for Health Affairs through the Hearing Restoration Research Program under award number W81XWh-20-1-0484; and a grant to the APS by the USDOE, Basic Energy Sciences, Office of Science under contract No. W-31-109-ENG-38. We thank Microlumen for the polyimide catheter generous gift.

CRediT authorship contribution statement

FD: data curation; formal analysis; investigation; writing original draft, review, and editing. DW: Conceptualization, formal analysis, funding acquisition; project administration; supervision; validation; visualization; writing-review and editing; CPR: surgery, investigation, methodology; writing-review and editing

Data availability

All data analyzed have been shown in the paper. The raw data are available upon request from the corresponding author.

Declaration of interest

None of the authors declare a conflict of interest.

Declaration of generative AI in scientific writing

No AI and AI-assisted technologies were used in the writing process of the manuscript.

Submission declaration and verification

The work described has not been published previously, except as an abstract and poster for the Midwinter Meeting of the Association for Research in Otolaryngology (ARO) in San Jose in 2020. It is not under consideration for publication elsewhere. All authors approved the manuscript, and if accepted, it will not be published elsewhere in the same form, in English, or any other language, including electronically, without the written consent of the copyright holder.

Supporting information

Supplementary data associated with this article can be found in the online version at <TBD>

References

1. El Kechai, N. *et al.* Recent advances in local drug delivery to the inner ear. *Int J Pharm* **494**, 83-101, doi:10.1016/j.ijpharm.2015.08.015 (2015).
2. Salt, A. N. & Plontke, S. K. Local inner-ear drug delivery and pharmacokinetics. *Drug Discov Today* **10**, 1299-1306, doi:10.1016/S1359-6446(05)03574-9 (2005).
3. Li, Y. *et al.* Comparison of inner ear drug availability of combined treatment with systemic or local drug injections alone. *Neurosci Res* **155**, 27-33, doi:10.1016/j.neures.2019.07.001 (2020).
4. Chen, Y. *et al.* Endoscopic intratympanic methylprednisolone injection for treatment of refractory sudden sensorineural hearing loss and one case in pregnancy. *J Otolaryngol Head Neck Surg* **39**, 640-645 (2010).
5. Dormer, N. H., Nelson-Brantley, J., Staecker, H. & Berkland, C. J. Evaluation of a transtympanic delivery system in Mus musculus for extended release steroids. *Eur J Pharm Sci* **126**, 3-10,

doi:10.1016/j.ejps.2018.01.020 (2019).

6. Hoffer, M. E. *et al.* Transtympanic versus sustained-release administration of gentamicin: kinetics, morphology, and function. *Laryngoscope* **111**, 1343-1357, doi:10.1097/00005537-200108000-00007 (2001).
7. Li, L., Ren, J., Yin, T. & Liu, W. Intratympanic dexamethasone perfusion versus injection for treatment of refractory sudden sensorineural hearing loss. *Eur Arch Otorhinolaryngol* **270**, 861-867, doi:10.1007/s00405-012-2061-0 (2013).
8. Plontke, S. K., Zimmermann, R., Zenner, H. P. & Lowenheim, H. Technical note on microcatheter implantation for local inner ear drug delivery: surgical technique and safety aspects. *Otol Neurotol* **27**, 912-917, doi:10.1097/01.mao.0000235310.72442.4e (2006).
9. Sale, P. J. P. *et al.* Cannula-based drug delivery to the guinea pig round window causes a lasting hearing loss that may be temporarily mitigated by BDNF. *Hear Res* **356**, 104-115, doi:10.1016/j.heares.2017.10.004 (2017).
10. Maini, S. *et al.* Targeted therapy of the inner ear. *Audiol Neurootol* **14**, 402-410, doi:10.1159/000241897 (2009).
11. Murillo-Cuesta, S. *et al.* Direct drug application to the round window: a comparative study of ototoxicity in rats. *Otolaryngol Head Neck Surg* **141**, 584-590, doi:10.1016/j.otohns.2009.07.014 (2009).
12. Sheppard, W. M., Wanamaker, H. H., Pack, A., Yamamoto, S. & Slepecky, N. Direct round window application of gentamicin with varying delivery vehicles: a comparison of ototoxicity. *Otolaryngol Head Neck Surg* **131**, 890-896, doi:10.1016/j.otohns.2004.05.021 (2004).
13. Zhang, Y. *et al.* Comparison of the distribution pattern of PEG-b-PCL polymersomes delivered into the rat inner ear via different methods. *Acta Otolaryngol* **131**, 1249-1256, doi:10.3109/00016489.2011.615066 (2011).
14. Jero, J., Tseng, C. J., Mhatre, A. N. & Lalwani, A. K. A surgical approach appropriate for targeted cochlear gene therapy in the mouse. *Hear Res* **151**, 106-114, doi:10.1016/s0378-5955(00)00216-1 (2001).
15. Farrah, A. Y., Al-Mahallawi, A. M., Basalious, E. B. & Nesseem, D. I. Investigating the Potential of Phosphatidylcholine-Based Nano-Sized Carriers in Boosting the Oto-Topical Delivery of Caroverine: in vitro Characterization, Stability Assessment and ex vivo Transport Studies. *Int J Nanomedicine* **15**, 8921-8931, doi:10.2147/IJN.S259172 (2020).
16. Zhang, L. *et al.* Understanding the translocation mechanism of PLGA nanoparticles across round window membrane into the inner ear: a guideline for inner ear drug delivery based on nanomedicine. *Int J Nanomedicine* **13**, 479-492, doi:10.2147/IJN.S154968 (2018).
17. Glueckert, R., Pritz, C. O., Roy, S., Dudas, J. & Schrott-Fischer, A. Nanoparticle mediated drug delivery of rolipram to tyrosine kinase B positive cells in the inner ear with targeting peptides and agonistic antibodies. *Front Aging Neurosci* **7**, 71, doi:10.3389/fnagi.2015.00071 (2015).

18. Maina, J. W. *et al.* Mold-templated inorganic-organic hybrid supraparticles for codelivery of drugs. *Biomacromolecules* **15**, 4146-4151, doi:10.1021/bm501171j (2014).
19. Paasche, G., Bogel, L., Leinung, M., Lenarz, T. & Stover, T. Substance distribution in a cochlea model using different pump rates for cochlear implant drug delivery electrode prototypes. *Hear Res* **212**, 74-82, doi:10.1016/j.heares.2005.10.013 (2006).
20. Paasche, G. *et al.* Technical report: modification of a cochlear implant electrode for drug delivery to the inner ear. *Otol Neurotol* **24**, 222-227, doi:10.1097/00129492-200303000-00016 (2003).
21. Brown, J. N., Miller, J. M., Altschuler, R. A. & Nuttall, A. L. Osmotic pump implant for chronic infusion of drugs into the inner ear. *Hear Res* **70**, 167-172, doi:10.1016/0378-5955(93)90155-t (1993).
22. Richter, C. P. *et al.* Fluvastatin protects cochleae from damage by high-level noise. *Sci Rep* **8**, 3033, doi:10.1038/s41598-018-21336-7 (2018).
23. O'Leary, S. J., Klis, S. F., de Groot, J. C., Hamers, F. P. & Smoorenburg, G. F. Perilymphatic application of cisplatin over several days in albino guinea pigs: dose-dependency of electrophysiological and morphological effects. *Hear Res* **154**, 135-145, doi:10.1016/s0378-5955(01)00232-5 (2001).
24. Kim, J. & Ricci, A. J. A chemo-mechanical cochleostomy preserves hearing for the in vivo functional imaging of cochlear cells. *Nat Protoc* **18**, 1137-1154, doi:10.1038/s41596-022-00786-4 (2023).
25. Plontke, S. K. & Salt, A. N. Local drug delivery to the inner ear: Principles, practice, and future challenges. *Hear Res* **368**, 1-2, doi:10.1016/j.heares.2018.06.018 (2018).
26. Mader, K., Lehner, E., Liebau, A. & Plontke, S. K. Controlled drug release to the inner ear: Concepts, materials, mechanisms, and performance. *Hear Res* **368**, 49-66, doi:10.1016/j.heares.2018.03.006 (2018).
27. Hao, J. & Li, S. K. Inner ear drug delivery: Recent advances, challenges, and perspective. *Eur J Pharm Sci* **126**, 82-92, doi:10.1016/j.ejps.2018.05.020 (2019).
28. Nyberg, S., Abbott, N. J., Shi, X., Steyger, P. S. & Dabdoub, A. Delivery of therapeutics to the inner ear: The challenge of the blood-labyrinth barrier. *Sci Transl Med* **11**, doi:10.1126/scitranslmed.aao0935 (2019).
29. Tandon, V. *et al.* Microfabricated reciprocating micropump for intracochlear drug delivery with integrated drug/fluid storage and electronically controlled dosing. *Lab Chip* **16**, 829-846, doi:10.1039/c5lc01396h (2016).
30. Lee, M. Y. *et al.* Dexamethasone delivery for hearing preservation in animal cochlear implant model: continuity, long-term release, and fast release rate. *Acta Otolaryngol* **140**, 713-722, doi:10.1080/00016489.2020.1763457 (2020).
31. Hu, B., Salvi, R. J. & Henderson, D. [The technique of chronic infusion of drugs into the cochlea by an osmotic pump]. *Zhonghua Er Bi Yan Hou Ke Za Zhi* **33**, 169-171 (1998).
32. Kim, E. S. *et al.* A microfluidic reciprocating intracochlear drug delivery system with reservoir and active dose control. *Lab Chip* **14**, 710-721, doi:10.1039/c3lc51105g (2014).

33. Chen, Z., Mikulec, A. A., McKenna, M. J., Sewell, W. F. & Kujawa, S. G. A method for intracochlear drug delivery in the mouse. *J Neurosci Methods* **150**, 67-73, doi:10.1016/j.jneumeth.2005.05.017 (2006).
34. Council, N. R. Guide for the Care and Use of Laboratory Animals. *Eighth Edition, Washington DC: The National Academies Press.(https://doi.org/10.17226/12910* (2011).
35. Stokes, E. L., Flecknell, P. A. & Richardson, C. A. Reported analgesic and anaesthetic administration to rodents undergoing experimental surgical procedures. *Lab Anim* **43**, 149-154, doi:10.1258/la.2008.008020 (2009).
36. Clark, T. S., Clark, D. D. & Hoyt, R. F., Jr. Pharmacokinetic comparison of sustained-release and standard buprenorphine in mice. *J Am Assoc Lab Anim Sci* **53**, 387-391 (2014).
37. Gaskill, B. N., Karas, A. Z., Garner, J. P. & Pritchett-Corning, K. R. Nest building as an indicator of health and welfare in laboratory mice. *J Vis Exp*, 51012, doi:10.3791/51012 (2013).
38. Langford, D. J. *et al.* Coding of facial expressions of pain in the laboratory mouse. *Nat Methods* **7**, 447-449, doi:10.1038/nmeth.1455 (2010).
39. Miller, A. L. & Leach, M. C. The Mouse Grimace Scale: A Clinically Useful Tool? *PLoS One* **10**, e0136000, doi:10.1371/journal.pone.0136000 (2015).
40. Graf, R., Cinelli, P. & Arras, M. Morbidity scoring after abdominal surgery. *Lab Anim* **50**, 453-458, doi:10.1177/0023677216675188 (2016).
41. Oliver, V. L., Thurston, S. E. & Lofgren, J. L. Using Cageside Measures to Evaluate Analgesic Efficacy in Mice (Mus musculus) after Surgery. *J Am Assoc Lab Anim Sci* **57**, 186-201 (2018).
42. Paganin, D. & Nugent, K. A. Noninterferometric phase imaging with partially coherent light. *Phys. Rev. Lett.* **80**, 2586-2589 (1998).
43. Paganin, D., Mayo, S. C., Gureyev, T. E., Miller, P. R. & Wilkins, S. W. Simultaneous phase and amplitude extraction from a single defocused image of a homogeneous object. *J. Microsc.* **206**, 33-40 (2002).
44. Weitkamp, T., Haas, D., Wegrzynek, D. & Rack, A. ANKAphase: software for single-distance phase retrieval from inline X-ray phase-contrast radiographs. *J. Synchrotron Rad.* **18**, 617-629 (2011).
45. Gursoy, D., De Carlo, F., Xiao, X. & Jacobsen, C. TomoPy: a framework for the analysis of synchrotron tomographic data. *Journal of synchrotron radiation* **21**, 1188-1193, doi:10.1107/S1600577514013939 (2014).
46. Ewald, A. J., Werb, Z. & Egeblad, M. Monitoring of vital signs for long-term survival of mice under anesthesia. *Cold Spring Harb Protoc* **2011**, pdb prot5563, doi:10.1101/pdb.prot5563 (2011).
47. Soken, H. *et al.* Mouse cochleostomy: a minimally invasive dorsal approach for modeling cochlear implantation. *Laryngoscope* **123**, E109-115, doi:10.1002/lary.24174 (2013).
48. Simon, F. *et al.* Surgical techniques and functional evaluation for vestibular lesions in the mouse: unilateral labyrinthectomy (UL) and unilateral vestibular neurectomy (UVN). *J Neurol* **267**, 51-61, doi:10.1007/s00415-020-09960-8 (2020).

49. Pham, T. M. *et al.* Housing environment influences the need for pain relief during post-operative recovery in mice. *Physiol Behav* **99**, 663-668, doi:10.1016/j.physbeh.2010.01.038 (2010).
50. Kuchinka, J. The Stapedial Artery in the Mongolian Gerbil (Meriones unguiculatus). *Anat Rec (Hoboken)* **301**, 1131-1137, doi:10.1002/ar.23801 (2018).
51. Emadi, G., Richter, C. P. & Dallos, P. Stiffness of the gerbil basilar membrane: radial and longitudinal variations. *J Neurophysiol* **91**, 474-488, doi:10.1152/jn.00446.2003 (2004).
52. Hawkley, T. F., Preston, M. & Maani, C. V. *Isoflurane*. (StatPearls Publishing, 2021).
53. Constantinides, C., Mean, R. & Janssen, B. J. Effects of isoflurane anesthesia on the cardiovascular function of the C57BL/6 mouse. *ILAR J* **52**, e21-31 (2011).
54. Jones, M. V., Brooks, P. A. & Harrison, N. L. Enhancement of gamma-aminobutyric acid-activated Cl- currents in cultured rat hippocampal neurones by three volatile anaesthetics. *J Physiol* **449**, 279-293, doi:10.1113/jphysiol.1992.sp019086 (1992).
55. Sheykholeslami, K., Megerian, C. A. & Zheng, Q. Y. Vestibular evoked myogenic potentials in normal mice and Phex mice with spontaneous endolymphatic hydrops. *Otol Neurotol* **30**, 535-544, doi:10.1097/MAO.0b013e31819bda13 (2009).
56. Willaert, A. *et al.* Vestibular dysfunction is a manifestation of 22q11.2 deletion syndrome. *Am J Med Genet A* **179**, 448-454, doi:10.1002/ajmg.a.7 (2019).
57. Honaker, J. A., Lee, C., Criter, R. E. & Jones, T. A. Test-retest reliability of the vestibular sensory-evoked potential (VsEP) in C57BL/6J mice. *J Am Acad Audiol* **26**, 59-67, doi:10.3766/jaaa.26.1.7 (2015).
58. Jones, T. A. *et al.* The adequate stimulus for mammalian linear vestibular evoked potentials (VsEPs). *Hear Res* **280**, 133-140, doi:10.1016/j.heares.2011.05.005 (2011).
59. Jones, S. M. *et al.* Hearing and vestibular deficits in the Coch(-/-) null mouse model: comparison to the Coch(G88E/G88E) mouse and to DFNA9 hearing and balance disorder. *Hear Res* **272**, 42-48, doi:10.1016/j.heares.2010.11.002 (2011).
60. Jones, S. M. *et al.* Stimulus and recording variables and their effects on mammalian vestibular evoked potentials. *J Neurosci Methods* **118**, 23-31, doi:10.1016/s0165-0270(02)00125-5 (2002).
61. Jones, T. A. & Jones, S. M. Short latency compound action potentials from mammalian gravity receptor organs. *Hear Res* **136**, 75-85, doi:10.1016/s0378-5955(99)00110-0 (1999).
62. Salt, A. N. & Hirose, K. Communication pathways to and from the inner ear and their contributions to drug delivery. *Hear Res* **362**, 25-37, doi:10.1016/j.heares.2017.12.010 (2018).
63. Stover, T., Yagi, M. & Raphael, Y. Transduction of the contralateral ear after adenovirus-mediated cochlear gene transfer. *Gene Ther* **7**, 377-383, doi:10.1038/sj.gt.3301108 (2000).
64. Roehm, P., Hoffer, M. & Balaban, C. D. Gentamicin uptake in the chinchilla inner ear. *Hear Res* **230**, 43-52, doi:10.1016/j.heares.2007.04.005 (2007).
65. Kho, S. T., Pettis, R. M., Mhatre, A. N. & Lalwani, A. K. Safety of adeno-associated virus as cochlear gene transfer vector: analysis of distant spread beyond injected cochleae. *Mol Ther* **2**, 368-373, doi:10.1006/mthe.2000.0129 (2000).

Figures

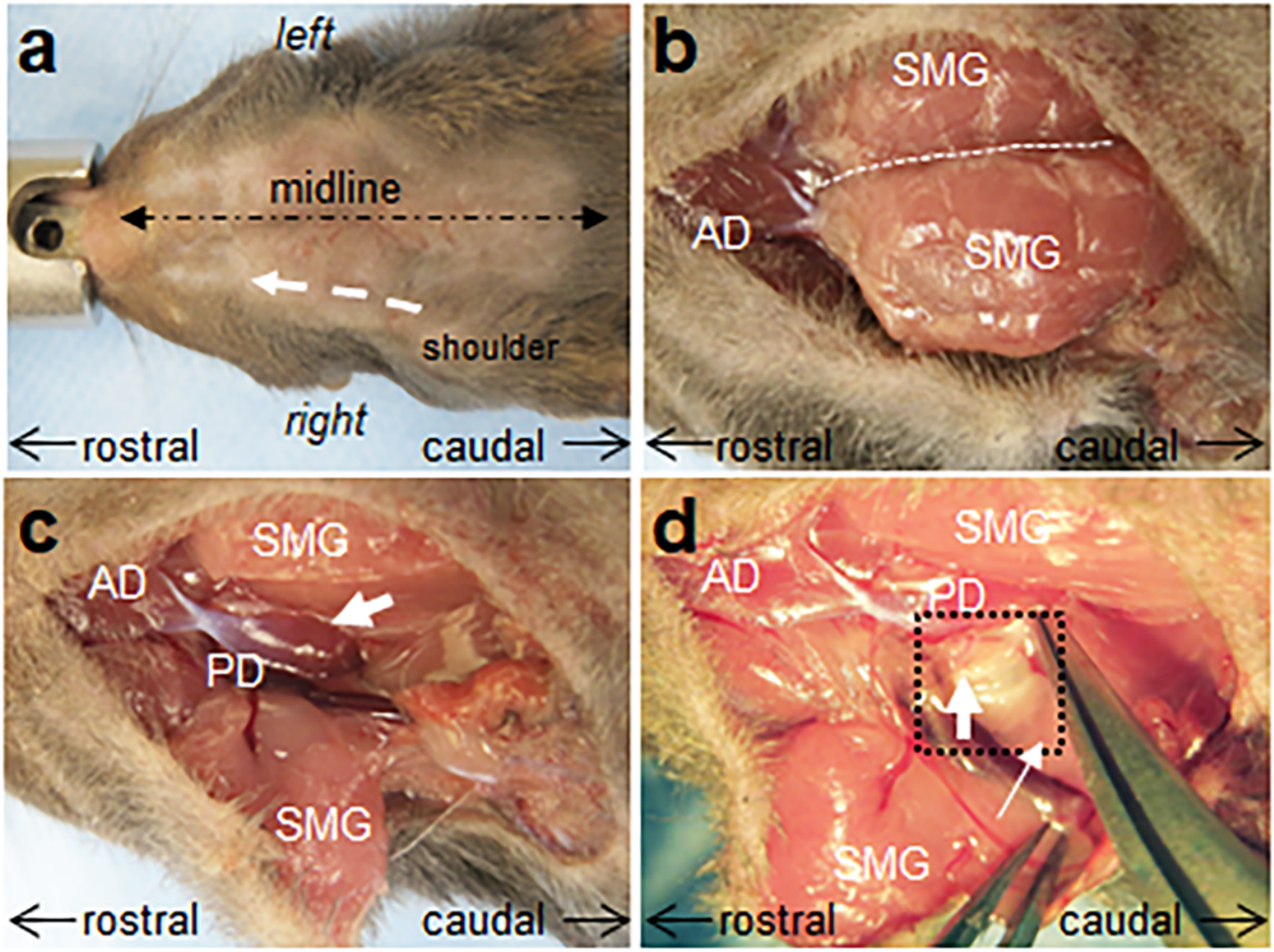

Figure 1

The surgical approach to the right bulla. **(a)** Place the mouse into the head holder and incise the skin along the white line, approximately 2 cm. **(b)** Retract the skin to expose the submandibular glands (SMG). Identify the anterior belly of the digastric muscle (AD). Separate the right and left SMG along the white dashed line by blunt dissection. **(c)** Retract the right SMG and identify the anterior and posterior belly of the digastric muscle, AD, and PD, respectively. The location of the bulla is below the PD (white arrow). **(d)** Detach and elevate the PD to expose the bulla region (box) and outer ear canal (thin white arrow). Avoid manipulating the facial nerve (thick arrow). Further, retract the muscles to expose the bulla.

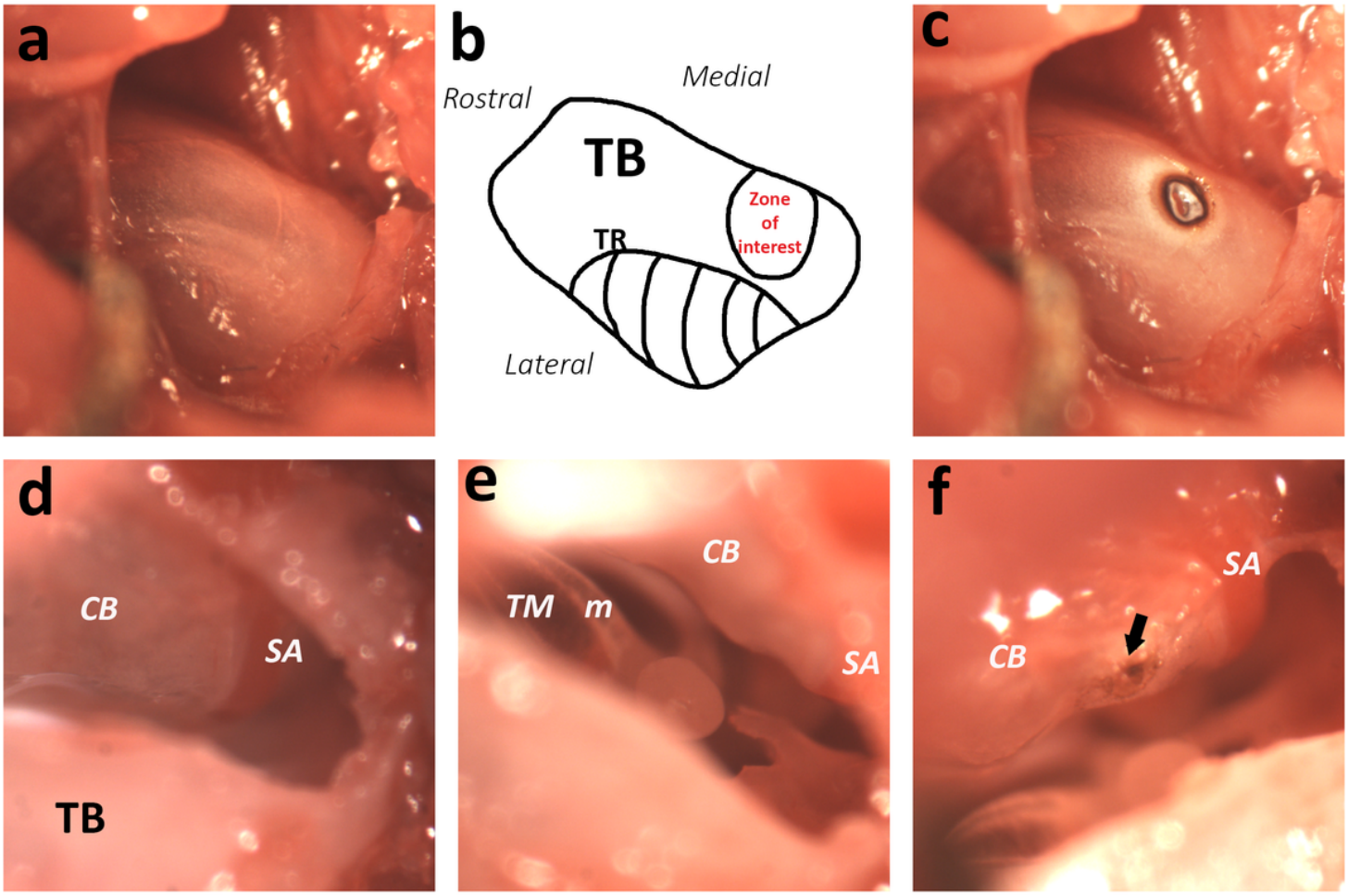

Figure 2

Opening of the bulla. **(a)** View and access to the bulla after retraction of the muscles. **(b)** shows a sketch of **(a),** providing the orientation of the field of view; identifiable structures are the tympanic bulla (TB), the tympanic ring (TR), and the zone of interest for the bullostomy. **(c)** An approximately 200 µm opening in the bulla is made with the CO_2 Laser by delivering a 100 ms single pulse at a 5 W power setting. **(d)** This opening is then widened with fine-pointed forceps (Supplemental Figure 2 and Supplemental Table 2: Tool #5) until the basal cochlear turn is visible. The stapedial artery (SA) denotes the stapedial artery, and (CB) the cochlear bone. **(e)** The mouse head is rotated to visualize the malleus (m) and tympanic membrane (TM). **(f)** is the image of a 100 µm cochleostomy created with the CO_2 Laser by delivering a single 100 ms single pulse at a 7 W power setting. The malleus and tympanic membrane can be identified.

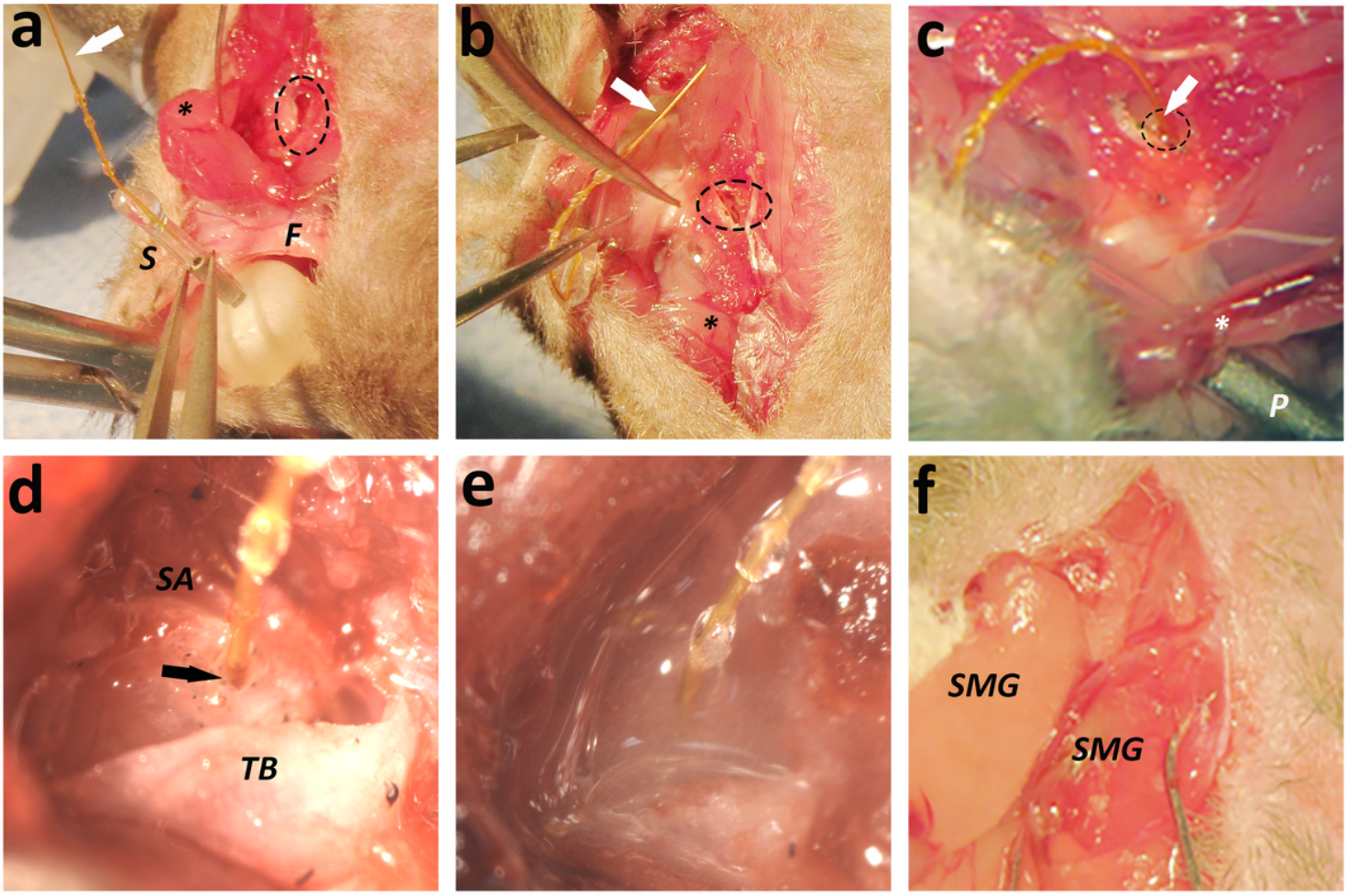

Figure 3

Osmotic pump placement. **(a)** A subdermal pocket is formed over the shoulder by separating the fascia (label "F") from the skin (label "S") using a pointed scissor (Supplemental Figure 2 and Table 2; tool #11), allowing the insertion and final ALZET® pump placement. It is important to remove the retractor before inserting the pump to prevent tissue damage by the retractor. Elevation of the sternocleidomastoid muscle (star) accommodates the pump's catheter (white arrow). The dashed circle encircles the bulla. **(b)-(c)** After insertion of the pump, the catheter (white arrow) is carefully bent with forceps toward the bulla (dashed circle). Sternocleidomastoid muscle (star) **(d)**. The catheter tip is placed through the hole of the cochleostomy (Black arrow). The cochleostomy is slightly larger than the catheter's diameter, and no additional tissue is placed to seal the opening. The dashed circle highlights the cochleostomy region where the catheter is inserted. **(e)** The catheter is stabilized in its position by filling the middle ear cavity with dental acrylic. **(f)** The tissue covering the bulla limits tissue desiccation during the 5 minutes of the acrylic polymerization time (Submandibular glands labeled as SMG).

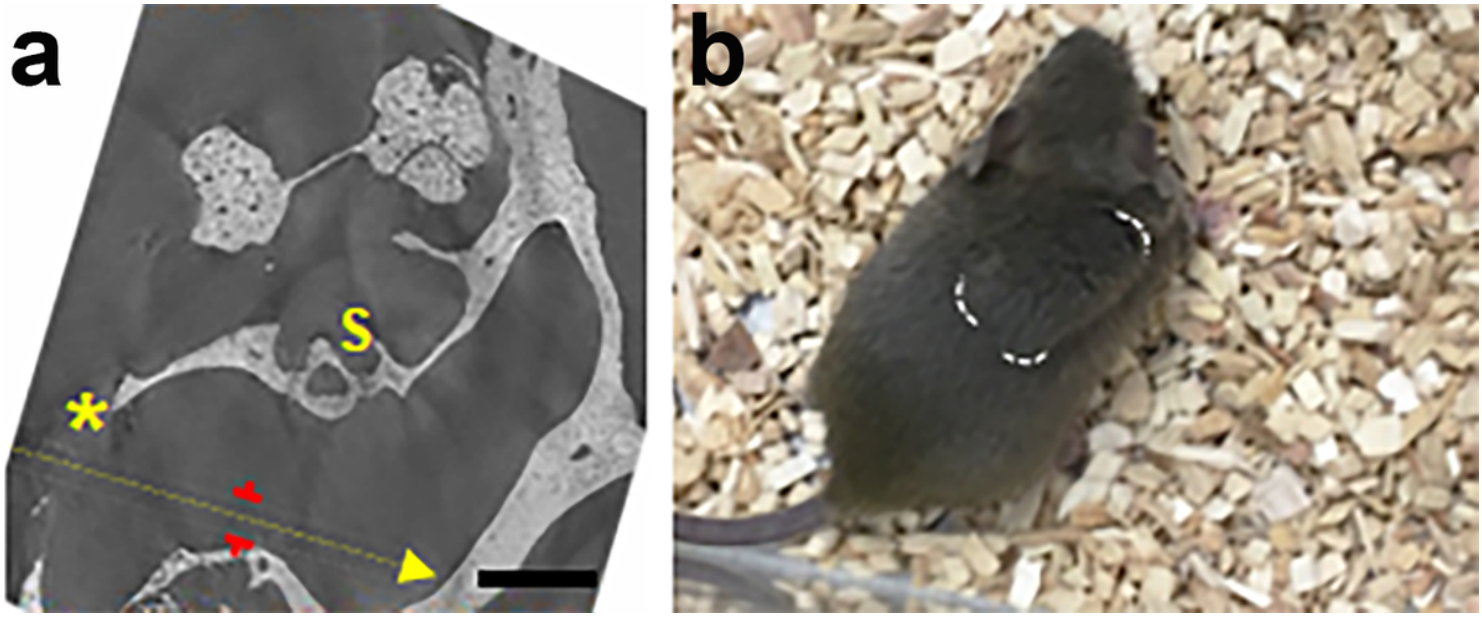

Figure 4

Post-surgical recovery. **(a)** Micro-computed tomography (micro-CT) images of the catheter placement obtained at the end of the study. The distal opening of the catheter is below the stapes footplate (S) in scala vestibuli. Fibrous tissue seals the cochleostomy (yellow star). The yellow dashed arrow highlights the center of the catheter tubing. The two red ( )signs delimited the exterior of the catheter walls (outer diameter 130 µm, the inner diameter 100 µm). (**b**) Top view of an implanted mouse. This mouse was sternal 4 min post-surgery and moved freely with no visible vestibular effects or impediments to ambulation (Supplemental Video 1). White dashed lines delimit the shape of implanted pump.

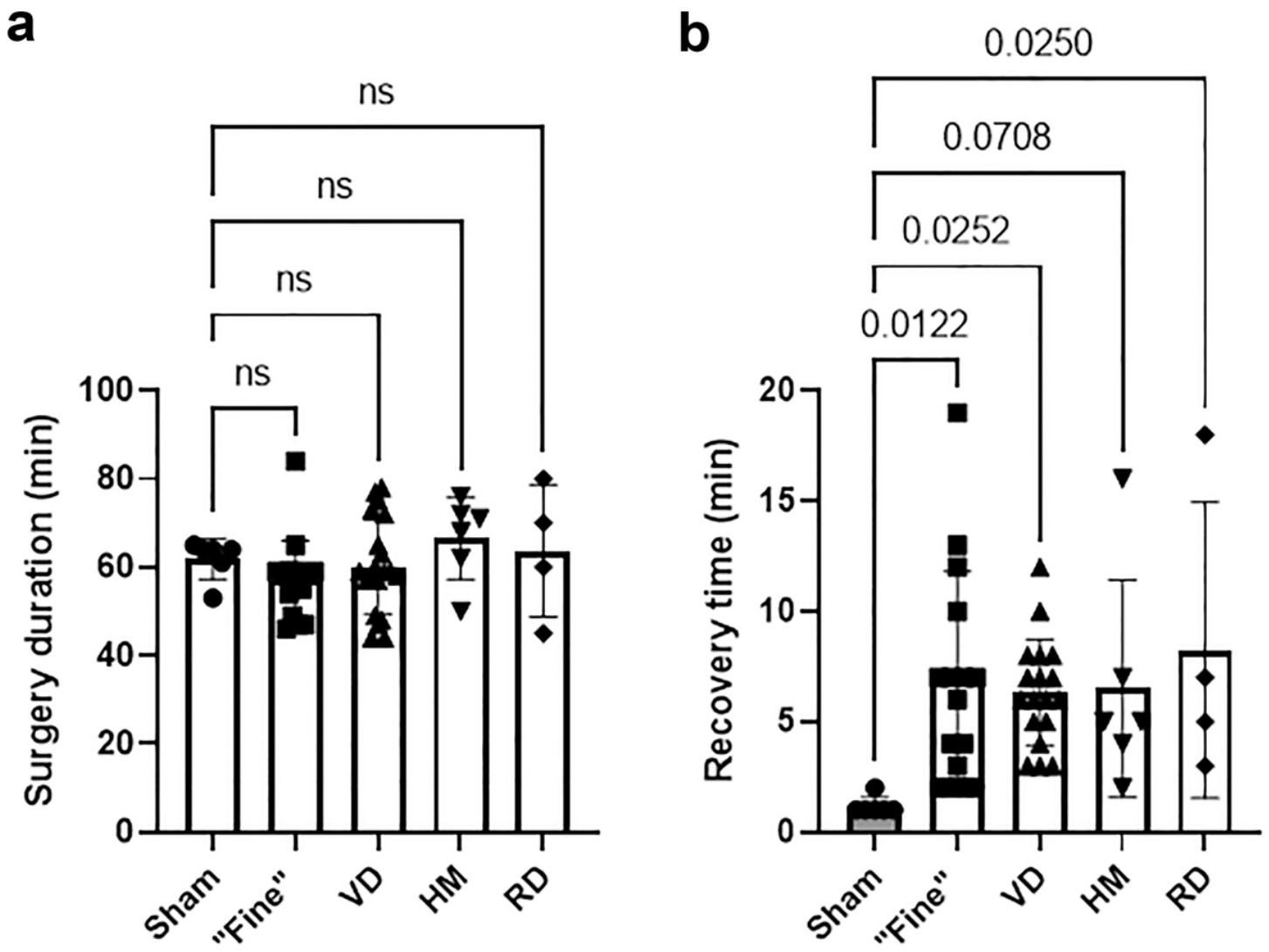

Figure 5

Reduced breathing rates (RD), bleeding (HM), and vestibular symptoms (VD) did not increase surgical **(a)** or recovery **(b)** times when compared to mice with no such events, classified in the figure as “Fine” or sham (exposed to anesthesia only). Moreover, mice undergoing surgery significantly increased recovery time compared to sham (anesthesia-only) mice. The surgery duration is between switching the anesthesia machine to the “ON” and the “OFF” position. Recovery from anesthesia is the time the mouse requires to move from a supine to a sternal position. Statistical analysis using GraphPad Prism version 9.5.1. Statistical analysis using One-way ANOVA for multiple comparisons. Graphs show means ± Standard Deviation (SD). P values are indicated on top of the brackets; ns = not significant.

Supplementary Files

This is a list of supplementary files associated with this preprint. Click to download.

- SupplementalinformationOsmoticpumpimplantation.docx

- Postsurgeryrecovery.mov

SA153. Statins Protect Mice From Noise-Induced Hearing Loss Frédéric Dépreux1 , Lyubov Czech1 , Yingjie Zhou1 , Claus-Peter Richter1 , Donna Whitlon*1 1Northwestern University, The Feinberg School of Medicine Category: Inner Ear: Damage and Protection Background: Previously, we demonstrated in guinea pigs that the HMG-CoA reductase inhibitor fluvastatin protects against noise-induced hearing loss (NIHL) when delivered directly to the contralateral cochlea. Guinea pigs exhibit a known variability in responses to noise. For this reason, and for future genetic experiments to study the mechanisms of statin protection, we move to an inbred mouse model, CBA/CaJ, which has been more consistent in noise induced auditory brain stem response (ABR) thresholds. We tested three hypotheses: (1) changes in threshold after high decibel noise exposure are stable about one week after exposure, (2) fluvastatin delivered directly to the cochlea protects the contralateral cochlea from (NIHL), and (3) orally given lovastatin protects against NIHL. Methods: To determine when ABR thresholds become stable, we exposed the mice for 2 hours to bandpass filtered noise (8-16 kHz) at levels between 90-110 dB SPL. To study the protective effect of stains, we developed a laser method to cleanly and accurately create a cochleostomy for insertion of a cannula from a miniosmotic pump. Hearing damage was achieved through bandpass filtered noise (8-16 kHz) exposure at 110dB SPL for 2 hrs. Fluvastatin delivery was initiated at time of noise exposure. We compared the threshold shifts at 2 weeks after noise exposure between fluvastatin+vehicle (50 μM in the pump), n=12, vehicle alone treated (n=8); noise exposure alone (n=5); and unexposed mice (n=11). We tested oral lovastatin (n=13), protection against NIHL. Lovastatin (60mg/kg or 120 mg/kg) was delivered several days before, the day of and 1 day after noise. Statistics - ANOVA with Tukey posttest or two-tailed t-test. Results: ABR threshold shifts were stable 1 week after noise. Intracochlear delivered fluvastatin protects against NIHL in mice. ABR threshold shifts: Unexposed animals (n=11), did not vary more than 1dB over 4 weeks. At two weeks after noise, ABR threshold shifts for vehicle alone vs fluvastatin+vehicle (in dB) were: 32kHz, 39.4 +/-15.9 vs 12.3 =/- 8.9 (p= 0.0002); 16 kHz, 29.4 +/- 6.8 vs 11.9 +/- 11.7, (p=0.0002); 8 kHz, 16.9 +/- 11.3 vs 5.7 +/-9.5 (p=0.0118). Fluvastatin does not protect against degeneration of synapses. As expected, at 2 weeks past noise, animals given oral carrier alone, had ABR threshold shifts over 30 dB at 8, 16 and 32 kHz. Oral lovastatin (60 and 120 mg/kg) protects against NIHL. ABR threshold shifts (in dB) of the carrier (n=4) vs lovastatin (n=13) were: 32 kHz: 31.8+/-7.5 vs 28.5 +/-11.6 (p=0.271); 16 kHz: 46.3 +/- 7.5 vs 25.4 +/-18.0 (p=0.042); 8 kHz: 37.5+/- 10 vs 14.2 +/- 13.7 (p=.0072). Conclusions: Fluvastatin delivered directly to the mouse cochlea protects against NIHL in the contralateral cochlea. Protection by oral lovastatin is promising for future studies of drugs for hearing loss. (Support: ONR N00014-18-1-2508 and HRRP W81XWH-20-1-0484)